The Role of NHE8 in the Regulation of Renal Proximal Tubule Calcium Reabsorption

by

Shane Wiebe

A thesis submitted in partial fulfillment of the requirements for the degree of

Master of Science

Department of Physiology

University of Alberta

ABSTRACT

Abnormalities in calcium homeostasis can result in kidney stones, a painful and potentially life-threatening condition. Improved therapies for this disorder can only be achieved through increased fundamental knowledge about calcium handling. In the kidneys, filtered calcium (Ca^{2+}) is reabsorbed along the nephron. To delineate the renal regulation of calcium reabsorption, we performed a mRNA micro-array on kidneys from mice treated with the calcium sensing receptor (CaSR) agonist cinacalcet. This revealed that the sodium/hydrogen exchanger isoform 8 (NHE8) expression was decreased by the CaSR agonist. These results were confirmed by quantitative PCR. Administration of vitamin D to mice also decreased NHE8 mRNA expression. In contrast, immunoblotting demonstrated increased renal NHE8 protein expression from the same mice treated with cinacalcet or vitamin D. We therefore hypothesized that NHE8, similar to NHE3, plays a role in calcium homeostasis by facilitating the reabsorption of filtered calcium. To assess this, we first validated a renal cell culture model, normal rat kidney (NRK) cells. To this end, we demonstrated apical expression of NHE8 in NRK cells using surface biotinylation and confocal immunofluorescence microscopy. Functional studies demonstrate 5-(*N*-Ethyl-*N*-isopropyl) amiloride (EIPA) inhibitable NHE activity at concentrations minimally attenuating NHE1 activity in AP-1 cells. To delineate the molecular role of NHE8 in calcium homeostasis, we measured transepithelial $^{45}Ca^{2+}$ flux across confluent monolayers and $^{45}Ca^{2+}$ uptake in the presence and absence of EIPA. There was no difference between groups suggesting NHE8 does not participate in cellular Ca^{2+} handling. However, ratiometric calcium imaging, a technique with greater temporal resolution, revealed enhanced Ca^{2+} uptake with EIPA treatment and after removal of extracellular sodium. Together, these results suggest NHE8 mediates Ca^{2+} efflux from NRK cells either directly or in collaboration with other transport mechanisms.

ACKNOWLEDGEMENTS

First and foremost I would like to thank the Alexander lab. It has been an incredible privilege to work under the direction of Dr. Todd Alexander and alongside the phenomenal group of researchers, colleagues and friends in his lab. I will miss them dearly. This has been a learning experience and a chapter in my life I will never forget and can never replace. To my committee members Dr. Larry Fliegel and Dr. Emmanuelle Cordat, thank you for your guidance and feedback during my studies.

I also extend my gratitude to the Women's and Children Health Research Institute and the Stollery Children's Hospital Foundation for providing financial support for this research project and for the various training and learning sessions. This work would not have been possible without the financial support from the various research funding agencies including CIHR, AIHS, KFOC, and NSERC.

Thanks to the International Research Training Group and the Membrane Protein Disease Research Group for the opportunity to attend and present my work at seminars and the joint symposium in Germany. I have gained invaluable feedback and insight from all the members of these groups.

To everyone in the Department of Physiology, thank you for making my time here enriched in scientific discovery and fellowship. And finally, a special thanks to my family and friends for your unconditional support and encouragement through my academic and life journeys. This thesis is for you.

TABLE OF CONTENTS

TABLE OF FIGURES

TABLE OF ABBREVIATIONS

1α-OHase – 1α-Hydroxylase

ADHH – Autosomal dominant hypocalcemia with hypercalciuria

AUA – American Urological Association

APS – Ammonium Persulfate

BSA – Bovine serum albumin

$CaBP_{28k}$ – Calbindin-D_{28k}

CaSR – Calcium sensing receptor

CLDN – Claudin

cTAL – Cortical Thick Ascending Limb

DCT – Distal Convoluted Tubule

DKO – Double knock out ECaC – Epithelial calcium channel

EAU – European Association of Urology

ESRD – End-stage renal disease

EIPA – 5-(*N*-Ethyl-*N*-isopropyl) amiloride

GPCR – G-protein coupled receptor

HRP – Horse radish peroxidase

HSP – Heat shock protein

KD – Knock down

KO – Knock out

mTAL – Medullary Thick Ascending Limb

NCX – Sodium-calcium exchanger

NHE – Sodium-hydrogen exchanger

NKCC2 – Sodium, potassium, 2 chloride cotransporter

PCT – Proximal Convoluted Tubule

PMCA – plasma membrane calcium ATPase

PST – Proximal Straight Tubule

PTH – Parathyroid hormone

PVDF – Polyvinylidene difluoride

RPM – Revolutions per minute

RT – Room Temperature

SDS – Sodium dodecyl sulfate

SNP – Single nucleotide polymorphism

TAL – Thick Ascending Limb

TBST – Tris-Buffered Saline and Tween 20

TRPV5 – Transient receptor potential cation channel subfamily V member 5

VDR – Vitamin D receptor

VDRE – Vitamin D-responsive elements

CHAPTER 1: INTRODUCTION

1.1 Renal Physiology:

The evolution of multicellularity necessitated that organ systems evolve to work cooperatively in order to maintain physiologic homeostasis. The renal system, consisting of the kidneys, ureters, bladder, and urethra, is necessary for electrolyte homeostasis, acid-base balance, volume regulation, production of erythropoietin, and removal of toxins and metabolic wastes. The nephron, a tubular structure, is the functional unit of the kidney. Blood is filtered at the glomerulus and the ultrafiltrate enters Bowman's capsule while large molecules including proteins are retained in the blood. The filtrate then enters the first nephron segment known as the proximal tubule. The nephron is further divided into the Loop of Henle, the distal convoluted tubule (DCT), the connecting tubules (CNT), and the collecting duct. Each segment of the nephron is uniquely adapted to reabsorb or secrete specific ions and molecules according to physiologic needs. The filtrate remaining in the lumen eventually becomes urine and is excreted. Understanding how the kidneys orchestrate these complex processes is not trivial; however it is important since renal diseases are the 9th leading cause of death in the United States of America (Xu *et al.,* 2016). It is the goal of my MSc thesis to investigate the role of a potential molecular mediator of calcium reabsorption in the proximal tubule, NHE8.

1.2 The Proximal Tubule and Electrolyte Homeostasis:

Micropuncture analysis of dog and rat proximal tubules reveals that this segment is responsible for the reabsorption of roughly 67% of the glomerular ultrafiltrate (Bennett *et al.,* 1967; Ullrich *et al.,* 1963). Although never directly measured, it is assumed that the proximal tubule shares this capacity in human. The proximal tubule is considered a leaky epithelium

(Rector 1983), as it has a transepithelial electrical resistance (TEER) ranging from 5 to 20 $\Omega \bullet cm^2$ (LaPointe *et al.,* 1983) compared with the nearly 8000 $\Omega \bullet cm^2$ TEER of the bladder (Reuss and Finn 1974). This leakiness enables the proximal tubule to reabsorb ions via a paracellular pathway. Consistent with this, micropuncture analysis of canine nephron estimates that 67% of filtered calcium is reabsorbed via the paracellular pathway from the proximal tubule (Duarte and Watson 1967) and 10% of filtered magnesium (Cole and Quamme 2000). Further, significant reabsorption of monovalent ions occurs from the proximal tubule including 50% of filtered sodium (Mullins *et al.,* 2006), 80% of filtered bicarbonate, and 60% of filtered chloride (Choi *et al.,* 2000). The reabsorptive properties of the proximal tubule are largely dependent on the presence of apical transport proteins. Of particular importance to sodium, water, and bicarbonate reabsorption are the sodium/hydrogen exchangers (NHEs), which couple the transcellular transport of sodium to water movement down a concentration gradient (Mercer 1974). This process utilizes the energy of an electrochemical gradient established by the basolateral sodium/potassium ATPase (Preisig *et al.,* 1987; Baum 1992). Although the proximal tubule plays an important role in electrolyte homeostasis, the molecular mediators involved remain incompletely elucidated.

1.3 The Role of Sodium/Hydrogen Exchangers (NHEs) in the Kidneys:

1.3.1 Overview: Electrolyte and pH regulation are critical processes to sustain all forms of life from simple prokaryotes to multicellular eukaryotes. Both of these functions are carried out by NHEs: multi-pass integral membrane proteins catalyzing the exchange of sodium and protons (Orlowski and Grinstein 2004). In mammals, there are 13 known evolutionarily

conserved NHE isoforms (Brett *et al.,* 2005) constituting the SLC9 gene family. This family can be further subdivided into three subgroups: the SLC9A, SLC9B, and SLC9C (Donowitz *et al.,* 2013). The SLC9A subgroup, which is the focus of this discussion, encompasses two groups of isoforms: the plasmalemmal NHEs 1-5 (SLC9A1-5), and the intracellular NHEs 6-9 (SLC9A6-9) (Fuster and Alexander 2014). The structure and function of mammalian NHEs have been appreciated for decades (Yun *et al.,* 1995) but knowledge of their cellular and molecular roles in various organ systems is lacking, particularly for the intracellular isoforms. NHE1-4, and NHE8 are expressed in kidneys and their functional roles in renal physiology will be addressed here.

Renal NHE activity was first predicted in the late 1940s by Pitts and colleagues when they observed an increase in urinary acid excretion upon intravenous infusion of sodium phosphate (Pitts *et al.,* 1948). The authors suggest that tubular excretion of protons in exchange for luminal sodium would, in one step, satisfy the necessity for conservation of base, the excretion of acid and maintenance of electroneutrality. Nearly 30 years later, Murer and colleagues were the first investigators to demonstrate sodium/hydrogen exchange activity in the apical membrane of small intestine and kidney by conducting transport studies on isolated brush border membrane vesicles (Murer *et al.,* 1976). These studies would prove to be invaluable in the following years leading to the identification and cloning of the first mammalian NHE gene, *SLC9A1*.

1.3.2 SLC9A1 – NHE1: In 1982, Pouyssegur and colleagues identified an amiloride-sensitive NHE system necessary for regulation of cytosolic pH and cell proliferation (Pouyssegur *et al.,* 1982). NHE1 was later cloned, and the primary structure determined providing an important milestone in the identification of the mammalian NHEs (Sardet *et al.,* 1989). NHE1 is known as the "housekeeping" NHE due to its function and ubiquitous gene expression. Human

NHE1 is 815 amino acids and is encoded on chromosome 1 (1p35 - p36.1) (Mattei *et al.,* 1988). In rabbit and rat kidney, NHE1 is expressed in the basolateral membrane of multiple nephron segments (Biemesderfer *et al.,* 1992; Rutherford *et al.,* 1997). Although the role of renal NHE1 has not been fully elucidated, NHE1 knockout (KO) mice display a roughly 60% reduction in bicarbonate absorption from isolated microperfused medullary thick ascending limbs (mTALs) of the Loop of Henle implicating a role for NHE1 in renal bicarbonate reclamation (Good *et al.,* 2004). Although the mechanism is undefined, the action of NHE1 is likely to coordinate with NHE3 in transepithelial bicarbonate reabsorption (Good *et al.,* 2011). NHE1 activity has also been implicated in proximal tubule cell survival by inhibiting apoptosis (Abu Jawdeh *et al.,* 2011; Khan *et al.,* 2014; Bocanegra *et al.,* 2014).

1.3.3 SLC9A2 – NHE2: The 812 amino acid NHE2 isoform was first cloned in 1993 and northern blot analysis demonstrated mRNA expressed in the rat uterus, liver, stomach, large intestine, jejunum and ileum but no expression in kidneys (Collins *et al.,* 1993). In agreement with these results, Bookstein and colleagues found, using *in situ* hybridization, that NHE2 mRNA is highly expressed in jejunum, ileum, and ascending and descending colon epithelium but no detectable message was observed in the kidneys (Brookstein *et al.,* 1997). Renal localization and function of NHE2 became controversial in the following year since Chambrey and colleagues developed an antibody against an NHE2 oligopeptide and immunoblot analysis revealed NHE2 protein in apical plasma membrane factions isolated from rat renal cortex but not in basolateral membrane fractions (Chambrey *et al.,* 1998). Further characterization of NHE2 in mouse lymphocyte (LAP1) cells demonstrates functional NHE activity (Malakooti *et al.,* 1999). NHE2 was later shown by microperfusion of the DCT to play a role in bicarbonate reclamation as a reduction in bicarbonate flux in the presence of the NHE2 specific inhibitor Hoe-694 was

observed (Wang *et al.,* 2001). The NHE2 KO mouse model does not have an overt disease phenotype (Schultheis *et al.,* 1998), but these mice do present increased cortical renal renin content implicating a role for NHE2 in macula densa feedback control of renin secretion (Hanner *et al.,* 2008). Since this finding, no further work has been published on the role of NHE2 in renal physiology which remains unclear and controversial.

1.3.4 SLC9A3 – NHE3: In 1992, rat NHE3, identified almost exclusively in the renal cortex, was cloned and sequenced by two independent groups (Tse *et al.,* 1992; Orlowski *et al.,* 1992). PS120 cells, a hamster lung cell line lacking endogenous NHE expression, stably expressing exogenous NHE3 demonstrate functional NHE activity which is resistant to high doses of amiloride (Tse *et al.,* 1993). To identify the cellular and subcellular localization of NHE3 in rabbit kidneys, Biemesderfer and colleagues developed an NHE3-isoform specific antibody. Their subsequent immunocytochemical studies on rabbit kidney sections showed NHE3 expression in the brush border membrane of the proximal convoluted tubule (PCT) (Biemesderfer *et al.,* 1993). Further, electron microscopy immunolocalization studies found NHE3 protein both in the apical membrane and subapical vesicles of the PCT (Biemesderfer *et al.,* 1997).

In the proximal tubule, copious amounts of sodium, water and bicarbonate are reabsorbed (Rector 1983) and NHE3 is important in these processes (Bobulescu and Moe 2009). Consistent with this, NHE3 brush border membrane protein expression increases in response to metabolic acidosis (Wu *et al.,* 1996) and NHE3 KO mice, both global KO and proximal tubular specific KO, develop metabolic acidosis and excrete an alkaline urine (Schultheis *et al.,* 1998; Li *et al.,* 2013) implicating NHE3 in acid-base homeostasis. More recently, NHE3 has been implicated in renal and intestinal calcium reabsorption through its activity in sodium and water reabsorption

(Pan *et al.,* 2013; Rievaj *et al.,* 2013). Mice lacking NHE3 gene expression have increased fractional excretion of calcium, reduced intestinal calcium absorption, and develop osteopenia to maintain plasma calcium concentration. The role of NHE3 in proximal tubule calcium reabsorption will later be discussed in further detail.

1.3.5 SLC9A4 – NHE4: The cloning, amino acid sequence deduction, and mRNA tissue expression of rat NHE4 took place in 1992 concurrently with the identification of NHE3 (Orlowski *et al.,* 1992). Immunoblot characterization shows limited tissue expression of NHE4 in rat kidney, uterus, liver, heart, and skeletal muscle, but significant expression in the stomach (Pizzonia *et al.,* 1998). In the kidney, NHE4 is primarily expressed in the renal cortex and it is enriched in basolateral membrane fractions. Further studies found that NHE4 is expressed and functions in the basolateral membrane of rabbit macula densa where it has been suggested that NHE4 serves a role in sodium transport, intracellular pH and cell volume regulation (Peti-Peterdi *et al.,* 2000). Immunohistochemistry localization studies also found NHE4 protein expression in the basolateral membrane of rat thick ascending limb (TAL) and DCT (Chambrey *et al.,* 2001). The authors also demonstrate that NHE4 activity in these segments has a low sensitivity to intracellular pH and speculate that NHE4 is involved in ammonium transport across basolateral membranes. Additional evidence for this hypothesis was later provided by NHE4 KO mice, as these animals exhibit compensated hyperchloremic metabolic acidosis, an inability to excrete urinary ammonium after acid loading, and impaired transepithelial ammonia absorption in the TAL; a process necessary for ammonium excretion in the collecting duct (Bourgeois *et al.,* 2010). Taken together, these results support a role for NHE4 in basolateral ammonia absorption from the TAL.

1.3.6 SLC9A5 – NHE5: In 1995, human NHE5 was cloned and its expression observed in the testis, spleen, skeletal muscle but predominantly in the brain (Klanke *et al.,* 1995). Although the physiologic role of NHE5 in the nervous system is undetermined, in hippocampal cells it was shown that perturbation of NHE5 function induces spontaneous spine growth via altered cellular pH regulation (Diering *et al.,* 2011). Renal NHE5 expression has not been shown, but in a linkage and association analysis of polymorphisms in patients with end-stage renal disease (ESRD), there was a significant association for patients with polymorphic markers for NHE5 to have a renoprotective effect and reduced risk of ESRD (Yu *et al.,* 2000). Since these findings, no further studies have investigated the role of NHE5 in ESRD.

1.3.7 SLC9A6 – NHE6: This endomembrane isoform is ubiquitously expressed in recycling endosomes. Tissue expression determined by northern blot analysis found NHE6 is most abundantly expressed in brain, skeletal muscle, and heart (Numata *et al.,* 1998). Mutations in *SLC9A6* result in severe neurological abnormalities in humans (Gilfillan *et al.,* 2008) but its role in renal physiology is not known.

1.3.8 SLC9A7 – NHE7: First cloned and characterized in 2001, NHE7 is ubiquitously expressed in the *trans*-Golgi network where it mediated sodium or potassium influx in exchange for protons (Numata *et al.,* 2001). Its physiologic role in the Golgi has not been investigated but Onishi and colleagues found that NHE7 overexpression in a breast cancer cell line had enhanced tumor progression implicating a role in the oncogenic process (Onishi *et al.,* 2012). The role of NHE7 in renal physiology has not been investigated.

1.3.9 SLC9A8 – NHE8: NHE8 was first identified and cloned from mouse kidney in 2003 (Goyal *et al.,* 2003). Encoded by the gene *SLC9A8*, NHE8 is one of the most recently identified

and cloned mammalian NHEs and consequently, its cellular and physiologic function is one of the least understood (Refer to section 1.4 of this thesis for a full literature review of NHE8).

1.3.10 SLC9A9 – NHE9: Northern blot analysis of human tissue revealed widespread but not ubiquitous expression of *SLC9A9* with highest levels in the brain, heart, and skeletal muscle (Silva *et al.,* 2003). In the brain, NHE9 has been implicated in neurological disorders. Morrow and colleagues found NHE9 nonsense mutations in two unrelated patients with autistic disorder (Morrow *et al.,* 2008). Furthermore, functional evaluation of autism-associated mutations in NHE9 demonstrates that they lack function in astrocytes (Kondapalli *et al.,* 2013). In support of these findings, the NHE9 KO mouse demonstrates an autistic phenotype likely due to aberrant endosomal function and a mistrafficking of membrane neurotransmitter receptors (Yang *et al.,* 2016). NHE9 likely does not have a role in renal physiology but this possibility has not been formally investigated.

1.4 NHE8 Literature Review:

1.4.1 NHE8 History: NHE8, encoded by the gene *SLC9A8*, is one of the most recently identified and cloned mammalian NHEs and consequently, its cellular and physiologic function is one of the least understood. Prior to the identification of NHE8, Choi and colleagues observed in microperfused PCTs from mice with NHE3, NHE2 or both NHE3 and NHE2 deleted that there was only a 50% reduction in sodium-dependant proton secretion. The remaining 50% activity was lost with treatment of 100 μM 5-(*N*-Ethyl-*N*-isopropyl) amiloride (EIPA) suggesting the presence of another NHE isoform in the PCT contributing the remaining activity (Choi *et al.,* 2000). These results were surprising for two reasons: first, NHE2 localizes to the brush border

membrane of the PCT with NHE3 suggesting an involvement in apical sodium-hydrogen exchange. Second, NHE3 had been implicated as the main player in sodium reabsorption from the proximal tubule and although the results do not argue against this, 50% NHE activity remains in its absence. In addition, NHE3 KO neonates did not have difficulty to thrive, further suggesting the involvement of another player compensating the loss of NHE3. NHE2 and NHE3 were the only known NHE isoforms localizing to the apical membrane of the PCT at this time. However, the findings supported the presence of a third isoform and thus when visualized in the PCT, NHE8 was hypothesized to be contributing the remaining activity. In support of this, Becker and colleagues identified ontogeny of NHE8 in the rat proximal tubule whereby NHE8 brush border membrane protein expression is highest during neonatal development and decreases during maturation whereas NHE3 protein increases (Becker *et al.,* 2007). A compensatory role of NHE8 in the absence of NHE3 could therefore explain the ability of NHE3 KO neonatal mice to thrive.

1.4.2 The identification and localization of NHE8: NHE8 was first identified and cloned from mouse kidney in 2003 (Goyal *et al.,* 2003). The authors discovered a partial mRNA code through the TBLASTIN search of GenBank using NHE3 as a query. The full length mRNA was identified using a combination of 5' and 3' rapid amplification of cDNA end and nested PCR. Northern blot analysis revealed the presence of NHE8 mRNA in every human tissue particularly the heart, brain, spleen, lung, liver, skeletal muscle, kidney and testis demonstrating ubiquitous gene expression. Further, *in situ* hybridization of NHE8 revealed enriched message in the outer stripe of the renal outer medulla and the tubules surrounding juxtamedullary glomeruli, strongly indicating proximal tubule localization. The authors later validated these findings by developing an NHE8 specific monoclonal antibody (7A11) and observing PCT and proximal straight tubule

(PST) brush border membrane localization using immunofluorescence microscopy on rat kidney sections (Goyal *et al.,* 2005). During the same year, another group investigated the cellular localization and function of NHE8. First, using amino acid sequence alignment and hydrophybicity plot analysis, the authors derived a phylogenetic tree of mammalian NHE isoforms (Nakamura *et al.,* 2005). NHE8 was predicted to have 12 membrane-spanning domains with a cytosolic N- and C-terminus. Interestingly, the amino acid sequence similarity of NHE8 to other isoforms was generally low (between 23-27%) and was most similar to NHE9 which localizes to intracellular organelles. Importantly, the authors investigated the intracellular distribution of NHE8 in COS7 cells using immunofluorescence microscopy and concluded that NHE8 protein is localized to the Golgi and post-Golgi compartments. The functional role of NHE8 in the Golgi has not been well established. However, HeLa M-cells expressing a non-functional NHE8 mutant have altered endosomal morphology and function suggesting NHE8 may be involved in regulating protein trafficking via organelle acidification (Lawrence *et al.,* 2010). To investigate the cellular function of NHE8, Nakamura and colleagues purified NHE8 protein overexpressed in yeast and reconstituted NHE8 into artificial liposomes. Functional studies on this system suggest that NHE8 is a sodium/proton or potassium/proton exchanger *in vitro*. The authors noticed, however, that the NHE8 protein product extracted from yeast ran at a lower molecular weight on an SDS-PAGE compared to the calculated molecular mass of other eukaryotic NHEs suggesting this ortholog may have a slightly different structure and function than in mammals. Nevertheless, these results have provided important insight into the localization and function of NHE8.

1.4.3 The role of NHE8 in a mammalian cell model: To study NHE8 in a mammalian cell model, Zhang and colleagues characterized NHE8 in normal rat kidney (NRK) cells: a proximal

tubular derived cell that forms polarized monolayers (Zhang *et al.,* 2007). The authors demonstrated the presence of native NHE8 and NHE1 transcripts using reverse-transcriptase PCR and NHE8 apical membrane expression using confocal microscopy, cell surface biotinylation, and electron microscopy. Further, they found NHE activity on both the apical and basolateral surface of NRK cells which was reduced by small interfering RNA (siRNA) knockdown (KD) of either NHE8 or NHE1 respectively. This study provided evidence that NRK cells are a suitable model for studying endogenous mammalian NHE8 in cell culture.

1.4.4 The physiologic role of NHE8: The NHE8 KO mouse has reduced colon mucin synthesis and bicarbonate secretion (Xu *et al.,* 2012), an impaired ocular surface and altered eye morphology (Xu *et al.,* 2015), leydig cell dysfunction in the testes (Xu *et al.,* 2015), and aberrant intestinal mucosal integrity (Wang *et al.,* 2015). Interestingly, these mice do not have a kidney phenotype under normal or acidemic conditions. This is surprising since neonatal NHE3 KO mice have an increase in NHE8 PCT brush border membrane protein abundance and NHE activity with an acid load (Pirojsakul *et al.,* 2015). Since there is significant renal brush border membrane NHE activity in the NHE3 KO mice, Baum and colleagues investigated the physiological consequences of an NHE3/NHE8 double KO mouse. The authors found that single NHE8 KO mice had normal serum bicarbonate levels and pH, normal blood pressure and renal NHE activity compared with WT controls (Baum *et al.,* 2012). The authors suggest this is likely due to functional compensation by NHE3, since NHE3 brush border membrane protein expression is greater in the NHE8 KO mice. This would also explain the lack of renal phenotype in NHE8 KO mice. However, NHE8 does not seem to compensate for the loss of NHE3 via a similar mechanism since the NHE3 KO mice have significant metabolic acidosis, lower blood pressure, and reduced renal NHE activity despite increased NHE8 brush border membrane

protein abundance. These results suggest that NHE8 alone is unable to fully compensate for the loss of NHE3. Interestingly, the double knockout (DKO) mice have even lower blood pressure and renal NHE activity compared to the NHE3 KO mice. The authors concluded that NHE3 is the predominant mediator of NHE activity in the proximal tubule but NHE8 has a partial compensatory role in renal acidification and blood pressure maintenance in the absence of NHE3.

1.5 Calcium Handling by the Nephron:

1.5.1 Overview: Plasma calcium exists in three states: ionized, complexed to other ions, or bound to plasma proteins. Since ionized calcium orchestrates a variety of cellular processes including neural synaptic transmission, cell apoptosis, cell signaling, muscle contraction, and blood clotting, the body maintains extracellular calcium concentration within a very narrow range (Mundy and Guise 1999). In normal human physiology, calcium regulation occurs at three levels: intestinal absorption, bone deposition/resorption, and renal reabsorption/excretion (Renkema *et al.,* 2008). In the kidneys, reabsorption of filtered calcium occurs along the length of the nephron but the molecular mechanisms are generally poorly understood. In 1979 Wadi Suki discussed in detail what remains our current understanding of gross calcium transport in the nephron (Suki 1979). In brief, early micropuncture studies using the radioisotope calcium-45 indicate that roughly 60% of renal calcium reabsorption occurs in the PCT, 20% in the loop of Henle, 10% by the distal convoluted tubule, 5% by the collecting ducts and less than 5% is thus lost in the urine (Lassiter *et al.,* 1963). The ability of the collecting duct to reabsorb calcium is, however, controversial (Suki 1979; Bindels 1993) and will not be addressed in this discussion.

1.5.2 Calcium handling in the Proximal Tubule: Calcium reabsorption in the proximal tubule occurs via a passive process secondary to the absorption of sodium and water. This nephron segment has high calcium permeability as evinced by single nephron microperfusion experiments in rat tubules (Murayama *et al.,* 1972). In 1976, evidence was provided that supports a secondarily active process for proximal tubule calcium reabsorption rather than a passive process (Ullrich *et al*., 1976). The authors argue that a low transepithelial potential difference across the PCT does not account for the low ratio of luminal to peritubular capillary calcium levels observed. Instead, the authors show that calcium reabsorption is dependent on sodium since this process was inhibited when luminal sodium was replaced with choline or lithium, or in the presence of ouabain blocking active sodium reabsorption mediated by the sodium/potassium ATPase. Active transcellular flux of sodium was later demonstrated to provide the driving force for passive paracellular calcium reabsorption from the proximal tubule (**Figure 1C;** Ng *et al.,* 1984; Pitts *et al.,* 1988). In theory, at least two mechanisms could explain how active sodium reabsorption could mediate passive paracellular calcium flux. Firstly, the removal of luminal sodium would drive water reabsorption thereby concentrating luminal calcium and creating a concentration gradient that drives paracellular flux. Alternatively, the paracellular movement of water might interact with ionized calcium through intermolecular forces creating a convection current which has also been referred to as 'solvent drag' (Bomsztyk *et al.,* 1986; Charoenphandhu *et al.,* 2006; Tanrattana *et al.,* 2004; Tudpor *et al.,* 2008; Wright and Bomsztyk 1986). NHE3 is the predominant NHE in the proximal tubule expressed in the apical membrane (Orlowski *et al.,* 1992) and its function has provided the molecular link between sodium and calcium reabsorption in that segment (Pan *et al.,* 2012).

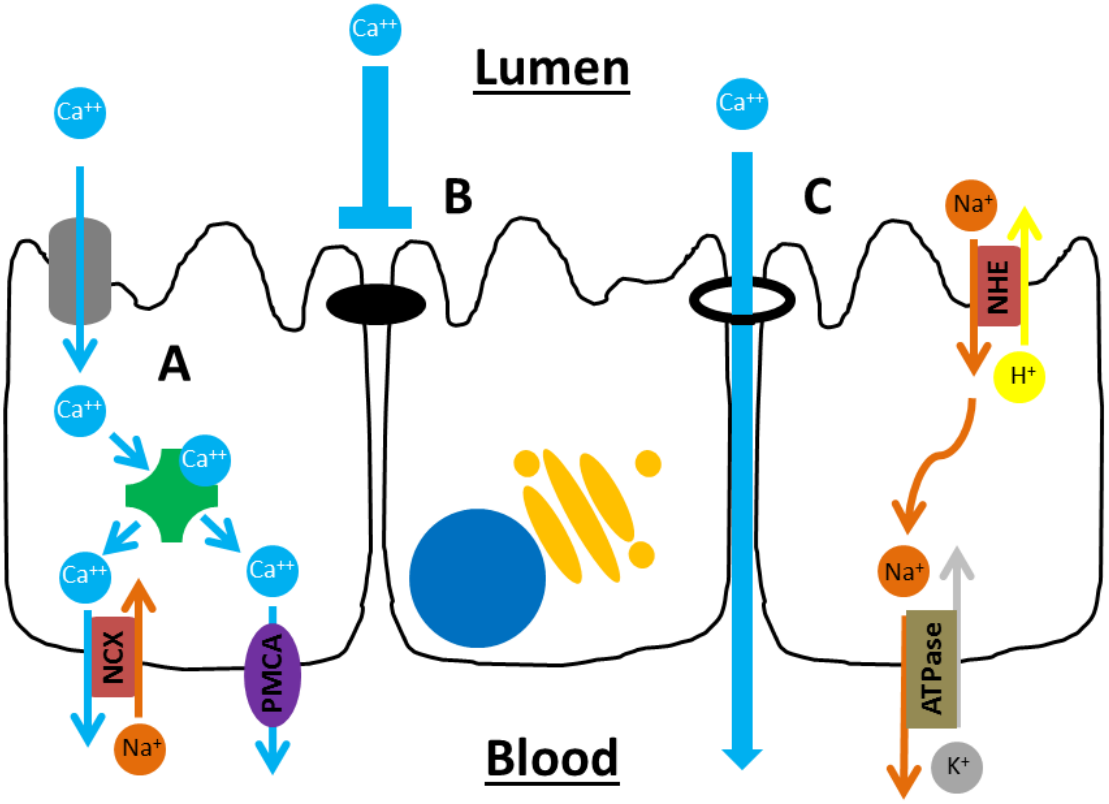

Figure 1) Mechanisms of renal transepithelial calcium reabsorption: Calcium is transported through epithelia via a transcellular route (A). Calcium first enters the cells through calcium channels and is then sequestered by calcium binding proteins. The calcium-calcium binding protein complex is then ferried from the apical to basolateral side of the cell where calcium is then released and exits the cell through either a NCX or a PMCA. Tight junctions between adjacent cells may act as a barrier for paracellular calcium reabsorption (B) or as a calcium-selective pore (C). For the latter, paracellular calcium reabsorption is dependent on the active transcellular reabsorption of sodium and water via the combined action of the basolateral sodium/potassium ATPase and apical membrane NHEs.

1.5.3 Calcium handling in the Thick Ascending Limb: Calcium reabsorption in the TAL occurs primarily through a paracellular mechanism driven by a large lumen positive transepithelial potential which is mostly generated by the action of the sodium, potassium, 2 chloride cotransporter (NKCC2) (Di Stefano *et al.,* 1993). This positive potential difference is diminished by treatment with furosemide, which leads to increased urinary excretion of calcium and magnesium (Lee *et al.,* 1994) and reduced reabsorption of these ions from microperfused rat TAL *in vivo* (Quamme 1981). The exact details of calcium reabsorption from the TAL are incompletely elucidated, however, certain claudins (CLDNs), which are tight junction proteins, expressed in this segment have been implicated in paracellular calcium reabsorption. Familial hypomagnesemia with hypercalciuria and nephrocalcinosis (FHHNC) is a human kidney disease characterized by renal calcium and magnesium wasting and progression to chronic renal failure (Hou *et al.,* 2008). Mutations in the tight junction proteins CLDN16 (Simon *et al.,* 1999) and CLDN19 (Konrad *et al.,* 2006) have been linked to this disease. More recently, it was demonstrated that CLDN14 is important for calcium reabsorption in the TAL (Dimke *et al.,* 2013). In this study, mice treated with active vitamin D (1,25-$(OH)_2D_3$) had a 10-fold increase in CLDN14 mRNA levels and a 40-fold increase when the mice were treated with the calcium sensing receptor (CaSR) agonist cinacalcet. These mice also had increased urinary calcium excretion thereby suggesting that CLDN14 is a paracellular blocker of calcium reabsorption from the TAL, whose expression in increased in response to increased calcium concentration in the blood (**Figure 1B;** Dimke *et al.,* 2013).

1.5.4 Calcium handling in the Distal Convoluted Tubule: In the distal nephron, calcium reabsorption occurs via active transcellular flux and accounts for roughly 10% of total calcium reabsorption from the filtered load (Bindels *et al.,* 1993). The channel central to this is the

transient receptor potential cation channel subfamily V member 5 (TRPV5) and it was first identified and cloned by Hoenderop and colleagues as a calcium selective channel (Hoenderop *et al.,* 1999; Muller *et al.,* 2000). TRPV5 is expressed in the proximal small intestine, the DCT of the nephron, and the placenta where it plays a critical role in calcium homeostasis. TRPV5, originally named the epithelial calcium channel 1 (ECaC1), is a member of the vanilloid receptor and transient receptor potential superfamily of calcium channels and is an integral membrane protein consisting of six transmembrane-spanning domains (Hoenderop *et al.,* 2002). The cellular mechanism by which transcellular calcium reabsorption occurs from the DCT is first by luminal entry through TRPV5, binding of calcium to Calbindin-D_{28K} ($CaBP_{28K}$), apical to basolateral diffusion of the calcium-$CaBP_{28k}$ complex, dissociation of calcium and extrusion though the sodium-calcium exchanger (NCX) or the plasma membrane calcium ATPase (PMCA) (**Figure 1A;** Hoenderop *et al*., 2000). The significance of TRPV5 function to calcium homeostasis is evident from the TRPV5 KO mouse model (Hoenderop *et al.,* 2003). The KO mouse has a nearly 3-fold increase in serum 1,25-$(OH)_2D_3$, a 6-fold increase in urinary calcium excretion, reduced femoral bone thickness and increased intestinal calcium reabsorption, allowing the mice to maintain a plasma calcium concentration comparable to wildtype. The dramatic compensatory changes caused by the loss of TRPV5 suggest that active transcellular calcium reabsorption from the distal nephron plays a critical role in whole-body calcium homeostasis. However, patients with mutations in TRPV5 have a milder phenotype (Muller *et al.,* 2002; Renkema *et al.,* 2009).

1.5.5 Calcium Sensing Receptor regulation of renal calcium transport: The CaSR has been cloned and functionally characterized in the parathyroid, kidney, nerve terminals, macrophages, and intestine (Brown *et al.,* 1993; Riccardi *et al.,* 1995; Ruat *et al.,* 1995;

Yamaguchi *et al.,* 1998; Chattopadhyay *et al.,* 1998). The CaSR is a G-protein coupled receptor (GPCR) which senses plasma calcium concentration and signals via activation of mitogen-activated protein kinases ultimately leading to alterations in gene expression for homeostatic regulation (Ward 2004). Cinacalcet is an FDA approved calcimimetic and acts via allosteric activation of the CaSR (Franceschini *et al.,* 2003). In the parathyroid gland, activation of the CaSR by ionized plasma calcium or cinacalcet leads to decreased secretion of parathyroid hormone (PTH) and subsequent reduction in plasma calcium levels (Torres 2006). In the kidneys, CaSR transcript has been identified from microdissected nephron segments including the glomeruli, PCT, PST, cTAL, mTAL, DCT, and the cortical and medullary colleting duct (Riccardi *et al.,* 1996). Further, immunofluorescence analysis revealed CaSR protein at the basolateral membrane of the cTAL, mTAL, macula densa, DCT, and at the brush border membrane of the PCT and PST (Riccardi *et al.,* 1998). Proximal tubule expression and localization of the CaSR is controversial since other investigators are unable to detect gene product there using reverse transcriptase PCR (Yang *et al.,* 1997). Nevertheless, these findings suggest that the CaSR plays a role in regulating renal calcium reabsorption from multiple nephron segments. Topala and colleagues demonstrated that the CaSR and TRPV5 co-localize in human DCT/CNT and that activation of the CaSR caused an increase in TRPV5 mediated calcium currents in HEK293 cells co-expressing TRPV5 and the CaSR (Topala *et al.,* 2009). Based on these findings, TRPV5 mediated calcium reabsorption is regulated by 1,25-$(OH)_2D_3$ through activation of the VDR as well as alterations in plasma calcium concentration via activation of the CaSR.

1.5.6 Vitamin D mediated regulation of renal calcium transport: 1,25-dihydroxy vitamin D (1,25-$(OH)_2D_3$) is an important regulator of physiologic calcium balance. It is synthesized in

the mitochondria of kidney proximal tubules by hydroxylation of 25-$(OH)D_3$ via 1α-Hydroxylase (1α-OHase) (Lawson *et al.,* 1971). After the identification of TRPV5 as the gatekeeper of active calcium reabsorption in the distal nephron, it was postulated that 1,25-$(OH)_2D_3$ likely acts to regulate TRPV5 expression directly. To test this hypothesis, the authors raised vitamin D-deficient rats and investigated changes in TRPV5 expression (Hoenderop *et al.,* 2001). In the vitamin D-deficient rats, RNAse protection assays revealed that kidney cortex TRPV5 mRNA levels were significantly reduced compared to control rats and expression returned to normal in replete rats. The vitamin D-depleted animals also had reduced plasma calcium levels which the authors suggest is due to reduction in TRPV5 expression. Similarly, in vitamin D receptor (VDR) KO mice, TRPV5 mRNA does not change in response to 1,25-$(OH)_2D_3$ injection, whereas in the WT mice, TRPV5 mRNA levels increase in a time and dose dependant fashion (Okano *et al.,* 2004). Further, Weber and colleagues screened the murine promoter sequence of TRPV5 and found a vitamin D-responsive element (VDRE) suggesting that TRPV5 gene expression can be regulated by activation of the VDR by 1,25-$(OH)_2D_3$ (Weber *et al.,* 2001). However, the authors of this study conclude that gene expression is not likely regulated by 1,25-$(OH)_2D_3$ but rather by the alterations in the concentration of plasma calcium through another mechanism. The presence of this controversy is due to experiments showing alterations in TRPV5 expression by diet-altered plasma calcium levels in mice with mutated VDR receptors unresponsive to changes in plasma 1,25-$(OH)_2D_3$. Further, evidence for 1,25-$(OH)_2D_3$ independent regulation of calcium transport mechanisms was provided when Hoenderop and colleagues developed a mouse model lacking the 1α-OHase and interrogated calcium handling in these animals (Hoenderop *et al.,* 2002). These mice present with a reduced serum calcium concentration, reduced mRNA and protein levels of TRPV5, $CaBP_{28k}$, NCX1, and PMCA1b compared to heterozygote littermates.

Interestingly, feeding these mice a calcium enriched diet restored plasma calcium levels as well as the expression of the above calcium transporting proteins independent of changes in plasma 1,25-$(OH)_2D_3$. Together, these results argue for a calcium-responsive element in the promoter regions of these calcium regulating proteins.

1.5.7 Parathyroid hormone regulation of renal calcium transport: Released from the parathyroid gland, parathyroid hormone (PTH) is important for elevating ionized plasma calcium concentration (Khosla *et al.,* 1993). Parathyroid chief cells sense changes in plasma calcium concentration by the CaSR which signals or inhibits the release of PTH depending on physiologic needs (Hoenderop *et al.,* 2005). In the kidneys, PTH increases expression of the DCT calcium transport machinery (van Abel *et al.,* 2005) via activation of the PTH/PTHrP receptor located in the DCT and other nephron segments (Riccardi *et al.,* 1996; Yang *et al.,* 1997). In proximal tubules, PTH acts to stimulate the activity of 1α-OHase thereby increasing 1,25-$(OH)_2D_3$ production, which in turn enhances intestinal calcium absorption (Hoenderop *et al.,* 2005). The role of PTH in calcium homeostasis is largely counterbalanced by the activity of calcitonin.

1.5.8 Calcitonin regulation of renal calcium transport: Calcitonin is a peptide hormone produced in the parafollicular cells of the thyroid gland and acts to reduce plasma calcium concentration but its role in regulating renal calcium transport is not well characterized (Friedman and Gesek 1995). In patients with primary hyperparathyroidism, treatment of 4 units/kg calcitonin resulted in reduced serum calcium and elevated urine calcium excretion (Cochran *et al.,* 1970) suggesting calcitonin is attenuating renal calcium reabsorption. These findings, among others, became controversial in the literature since it was later demonstrated that thyroparathyroidectomized rats receiving calcitonin at physiologic concentrations had reduced

urinary calcium excretion due to enhanced calcium reabsorption from the loop of Henle but a decline in plasma calcium concentration (Quamme 1980; Carney 1992). Adding to the controversy, Berndt and colleagues did not observe alterations in urinary calcium excretion in rabbits treated with calcitonin verses control (Berndt and Knox 1980). These differences have been ascribed to species heterogeneity (Eckermann-Ross 2008) but how calcitonin regulates renal calcium handling machinery is still undetermined.

1.6 Calcium Mishandling and Associated Pathophysiology:

1.6.1 Overview: Kidney stones, a painful and potentially life-threatening condition, are one of the oldest diseases known to medicine with descriptions of ancient treatment in Indian, Chinese, Babylonian and Greek texts (Eknoyan and De Santo 2012). However, the precise mechanism of kidney stone development is still poorly understood (Evan *et al.,* 2015). Kidney stone formation is complex and multifaceted involving dietary factors, genetic susceptibility, and environmental influences. The vast majority of kidney stones are calcium-containing where, by frequency of occurrence, 15-35% are calcium oxalate, 5-20% calcium phosphate, 40-45% mixed calcium oxalate/phosphate, 2-13% uric acid, 2-5% mixed calcium oxalate/uric acid, 10-15% struvite, 1-3% cysteine, and 0.5-1% ammonium urate (Favus 2013). Once a nucleation event occurs, crystals begin to form into stones until they reach a critical mass and dislodge from the kidneys into the ureter. Kidney stones are a common disorder where every year in the US alone more than a million patients require medical attention and more than 300,000 of those are emergency cases (Litwin 2012).

The prevalence of kidney stones in the US was 8.8% in 2012 (Scales *et al.,* 2012). There is a substantial economic burden associated with the disease. In 2000, outpatient physician visits for kidney stones cost $2.07 billion despite a 15% reduction in inpatient stays from 1994 (Pearle *et al.,* 2005). Kidney stones are not only painful, but stone episodes are associated with increases in adverse renal outcomes such as ESRD and cardiovascular disease (Alexander *et al.,* 2012 and 2014). The prevalence of nephrolithiasis (kidney stone formation) is also increasing over time. In the US, for individuals living in high-risk zones for nephrolithiasis, there is a predicted 16% increase in prevalence from 2010 to 2050 based on climate change models and unanticipated results of global warming (Brikowski *et al.,* 2008). There is also a 25% increase in nationwide cost associated with this increase in kidney stone prevalence. Increased fundamental knowledge about calcium handling is important to improve therapies for kidney stone patients and to create strategies to reduce the occurrence of stone development.

1.6.2 Hypercalciuria and Nephrolithiasis: Hypercalciuria is defined as an increase in urinary calcium excretion (above 0.1 mmol Ca/kg/day) and is caused by increased renal calcium filtration, reduction in renal calcium reabsorption or a combination of these factors (Peacock and Nordin 1968). However, in most cases, hypercalciuria is not attributed to increased renal calcium filtration as plasma calcium concentration is kept within a tight normal range for most patients (Henneman *et al.,* 1958). This suggests that impaired renal calcium reabsorption causes hypercalciuria. In 1939, Flocks was the first to describe a correlation between urinary calcium excretion and the development of ureteral calculi (Flocks 1939). Consequently, it has been observed that at least 50% of calcium oxalate stone formers have hypercalciuria making it a major risk factor for stone development (Lemann *et al.,* 1991).

1.6.3 Genetic factors influencing stone formation: Despite the large number of idiopathic calcium stone diagnoses, there are a variety of inherited disorders leading to stone development including adenine phosphoribosyltransferase (APRT) deficiency, autosomal dominant hypocalcemia with hypercalciuria (ADHH), Bartter syndrome, Dent's disease, familial hypomagnesemia with hypercalciuria and nephrocalcinosis (FHHNC), and primary hyperoxaluria (PH) (Edvardsson *et al.,* 2013). These disorders can also lead to chronic kidney disease (CKD) with progression to ESRD (Beara-Lasic *et al.,* 2011) but how these conditions affect renal calcium handling is largely undetermined. The inheritance pattern of kidney stones however, does not occur via mendelian inheritance but rather by a complex and polygenic fashion involving a variety of genes (Resnick *et al.,* 1968; McGeown 1960). Studying these genetic disorders has provided insight into a number of transport and regulatory processes central to renal electrolyte handling (Stechman *et al.,* 2009). For example, Dent's disease, an X-linked recessive disorder characterized by low molecular weight proteinuria, hypercalciuria, nephrocalcinosis, and nephrolithiasis (Dent and Freidman 1964), is commonly caused by mutations in the *CLCN5* gene encoding a chloride/proton antiporter (Fisher *et al.,* 1994). However, the mechanism by which *CLCN5* mutations lead to renal calcium mishandling is yet to be determined.

1.6.4 Treatment and management: Due to the fact that kidney stone episodes are largely idiopathic in nature, developing effective treatments is not straightforward. In 1983, potassium citrate was introduced as a treatment for kidney stones (Pak *et al.,* 1983), and since this discovery, no new drugs have been developed. Morgan and Pearle discuss in detail the current medical management of renal stones including screening, blood tests, urine analysis, radiographic imaging, metabolic testing, pharmacologic and dietary managements (Morgan and

Pearle 2016). The details are beyond the scope of this MSc thesis, however in summary, dietary and pharmacologic management is focused on reducing stone recurrence rates and stone prophylaxis. Dietary factors include increased fluid intake to reduce hypersaturation of the urine ultrafiltrate (Borghi *et al.,* 1999), increased calcium intake but reduced oxalate intake (Holmes and Assimos 2004). Increased citrate intake is recommended to reduce calcium precipitation and crystal aggregation (Zuckerman and Assimos 2009), reduce sodium intake to reduce renal calcium excretion (Nouvenne *et al.,* 2010), and reduce animal protein intake (Borghi *et al.,* 2002). The excessive use of vitamin C and calcium supplements also increases the risk of kidney stones, so they are discouraged (Traxer *et al.,* 2003; Curhan *et al.,* 1997/1999). Calcium and vitamin D supplements are known to increase the risk of stone development in postmenopausal women (Wallace *et al.,* 2011) but the effect of nutritional vitamin D intake in stone formers and the correlation between plasma vitamin D and stone development remains controversial (Tang and Chonchol 2013). For recurrent calcium based stones, thiazide diuretics have been recommended by the American Urological Association (AUA) and European Urological Association (EAU) for treatment (Pearle *et al.,* 2014). According to these guidelines, potassium citrate therapy is also offered to patients with recurrent calcium stones and low levels of urinary citrate.

1.7 Overall Rationale:

Diseases of the kidney are the 9th leading cause of death in the US (Xu *et al.,* 2016). The kidneys play a critical role in maintaining physiologic calcium homeostasis but aberrant calcium handling leads to kidney stones causing detrimental health consequences and an economic burden on health care. Understanding the cellular and molecular mechanisms of renal calcium

handling is the first step towards preventing and treating these conditions. The proximal tubule is responsible for the bulk of calcium reabsorption (~67%) but little is known about the mechanisms and regulators involved (Alexander *et al.,* 2013). NHE3 is a known regulator of proximal tubule calcium reabsorption in adult mice since the mouse KO model develop hypercalciuria, osteopenia, and a compensatory increase in intestinal calcium absorption from elevated plasma 1,25-$(OH)_2D_3$ (Pan *et al.,* 2012). NHE3 is the predominant NHE in the proximal tubule brush border membrane but NHE8 function partially compensates in its absence (Baum *et al.,* 2012) and there is increased NHE8 protein expression in the intestine of female NHE2X3 DKO mice (Xu *et al.,* 2011). NHE8 is ubiquitously expressed and localizes to the mid- to trans-Golgi but in the proximal tubule and in NRK cells it localizes to the apical brush border membrane where its function is poorly understood (Fuster and Alexander 2014; Zhang *et al.,* 2007). Using an mRNA microarray, the Alexander lab found that mice treated with cinacalcet, a CaSR agonist, have a roughly 50% reduction in NHE8 mRNA levels (Alexander lab unpublished data) suggesting a role for NHE8 in calcium homeostasis. The function of NHE8 as a mediator of calcium homeostasis has not been investigated. It is the goal of this thesis therefore to try to begin to understand the role of NHE8 in calcium homeostasis, and given its pattern of expression in the renal proximal tubule more specifically.

1.8 Hypothesis:

I hypothesize that NHE8 is driving transepithelial calcium reabsorption from the renal proximal tubule whereby NHE8 mediated sodium and subsequent water reabsorption establishes a concentration gradient driving calcium reabsorption.

CHAPTER 2: MATERIALS AND METHODS

2.1 Materials: Antibodies used for immunoblotting, and immunofluorescence include: Mouse anti-NHE8 7A11 monoclonal (Cat#: MA1-46357, Thermo Fisher Scientific, 81 Wayman Street, MA, USA), rabbit anti-NHE8 polyclonal (Cat#: NBP1-59888, Novus Biologicals, LLC 8100 Southpark Way, A-8 Littleton, CO, USA), mouse anti-HSP 25/27 monoclonal (Cat#: SMC-114D, Stressmarq Biosciences Inc, PO BOX 55036 Cadboro Bay, 3825 Cadboro Bay Rd, Victoria, BC, CAN), mouse anti-HSC 70 monoclonal (Cat#: SMC-151A, Stressmarq Biosciences Inc, PO BOX 55036 Cadboro Bay, 3825 Cadboro Bay Rd, Victoria, BC, CAN), and rabbit anti-HSP 90 polyclonal (Cat#: ADI-SPA-846, Enzo life Sciences Inc, 10 Executive Blvd, Farmingdale, NY, USA), and mouse anti-β-actin (Cat#: sc-47778, Santa Cruz Biotechnology, Inc, 10410 Finnell Street, Dallas, Texas, USA). To measure plasma membrane protein expression we used non-membrane permeable biotin reagent (EZ-Link Sulfo-NHS-Biotin, Cat#: 21331, Thermo Fisher Scientific, 81 Wayman Street, MA, USA). For measuring intracellular pH we used the pH sensitive ratiometric dye BCECF, AM (2',7'-Bis-(2-Carboxythyl)-5-(and-6)-Carboxyfluorescein, Acetoxymethyl Ester, Cat#: B1170 Molecular Probes, Thermo Fisher Scientific, 81 Wayman Street, MA, USA). For measuring intracellular calcium concentration we used the calcium sensitive ratiometric dye FURA-2, AM (Cat#: F1221 Molecular Probes, Thermo Fisher Scientific, 81 Wayman Street, MA, USA). For all experiments involving radioactive calcium, we used Calcium-45 radioisotope, 2 mCi stock (74 MBq, Cat#: NEZ013002MC, Perkin Elmer, 940 winter Street, Waltham, Massachesetts, USA). To inhibit NHE activity we used EIPA (5-(*N*-Ethyl-*N*-isopropyl) amiloride, Cat#: A3085 – 25 mg, Sigma-Aldrich, 2149, Winston Park Dr. Oakville, ON, CAN). We treated cells with Probenecid (Cat#: P-8761 Sigma-Aldrich, 2149, Winston Park Dr. Oakville, ON, CAN) while incubating with FURA-2 to inhibit fluorophore efflux. We purchased the following drugs from Sigma-Aldrich

(2149, Winston Park Dr. Oakville, ON, CAN) to block calcium channel function: Ruthenium Red (Cat#: R275-1), Verapamil (Cat#: V4629), and Felodipine (Cat#: F9677). Pluronic F-125 (Cat#: P3000MP, Molecular Probes, Thermo Fisher Scientific, 81 Wayman Street, MA, USA) was used to enhance FURA-2 uptake into NRK cells. To inhibit the GlcNAc phosphotransferase (GPT), we treated cells with tunicamycin (Cat#: T7765, Sigma-Aldrich). For western blot analysis, we transferred protein onto Immobilon polyvinylidene difluoride (PVDF) Transfer membrane (Cat#: IPVH00010, EMD Millipore, 109 Woodbine Downs Blvd, Unit 5, Etobicoke, ON, CAN). These membranes were visualized using the Carestream Molecular Imaging station (Carestream Health Inc. 150 Verona Street, Rochester, NY 14608). To measure protein and DNA concentrations, we used the Nanodrop 2000C Spectrophotometer (Cat#: ND-2000C, Thermo Fisher Scientific, 81 Wayman Street, MA, USA). For all experiments involving calcium-45 radionuclide, samples were dissolved in 4 ml scintillation fluid (ScintiSafe^{TM} Econo 1 Cocktail, Cat#: SX20-5, Fisher Chemical) and counted using a multipurpose scintillation counter (LS 6500 Beckman Coulter Inc. 4300 North Harbor Blvd, Fullerton, CA 92834, USA). Unless otherwise indicated, all reagents were purchased from Fisher Scientific.

2.2 Cell culture: Normal rat kidney (NRK) cells were purchased from American Type Culture Collection, Manassas, VA (NRK-52E ATCC CRL-1571). These are an adherent, polarized epithelial cell derived from *Rattus norvegicus* kidney proximal tubules (Zhang *et al.,* 2007). NRK cells were cultured in Dulbecco's Modified Eagle Medium (DMEM) with 4.5 g/L D-Glucose supplemented with 10% fetal bovine serum (FBS) and 1% Penicillin-Streptomycin-L-Glutamine (PSG) in a 37°C, 95% air and 5% CO_2 incubator. The FBS and antibiotics were removed from the cells during experiments. Cells were counted using a hemocytometer and

seeded at an appropriate and consistent density to be grown to confluence prior to experimentation. AP-1 cells are a mutant cell line derived from Chinese hamster ovaries. They have been used previously to characterize NHE1 activity (Jardet *et al.,* 1989) and were a kind gift from the Fliegel lab, Department of Biochemistry, University of Alberta.

2.3 Real-time PCR: Total RNA was isolated from kidneys using TRIzol Reagent (Invitrogen, Carlsbad, USA) per manufacturer's protocol. 1 μg of RNA was reverse transcribed by using Random Primers (Invitrogen) and SuperScript II reverse transcriptase (Invitrogen). Primers and probes used to evaluate expression of NHE8 were: mNHE8: forward primer 5'-CATGCTGGTGTTTGGAGAAAG-3'; probe 5'-TGGTGAGGACGATGGAGACTGC-3'; and reverse primer 5'-TTGTTAGACCTTCAGCCGTG-3'. As an internal control, mRNA levels of 18s were determined. Expression levels were quantified using the ABI Prism 7900 HT Sequence Detection System (Applied Biosystems, Foster City, CA, USA).

2.4 Immunoblotting: Cells were washed 3 times with 1x phosphate buffered saline (1x PBS) and lysed using radioimmunoprecipitation assay (RIPA) buffer (50 mM Tris Base, 150 mM NaCl, 1 mM EDTA, 1% Triton X-100, 0.1% SDS, 1% NP-40, 1/100 protease inhibitor cocktail [Calbiochem, Cat. No. 539134], 1/100 PMSA in double distilled water, adjusted to pH 7.4 with HCl), scrapped from the plate, collected, homogenized using a pestle mixer, and incubated on ice for 30 mins. Lysate was then centrifuged at 12, 000 revolutions per minute (RPM) for 20 mins at 4°C. The protein containing supernatant was collected and the pellet discarded. Using a nanodrop 2000c (Thermo Scientific), the 280 nm absorbance was measured and protein concentration calculated using a bovine serum albumin (BSA, Sigma-Aldrich A-

4503) standard curve. A known quantity of protein (depending on the experiment) was mixed with 2x Laemmli sample buffer (130 mM Tris-HCl pH 6.8, 4.6% SDS, 0.02% Bromphonel Blue, 20% Glycerol, 2% 2-Mercaptoethanol [Sigma-Aldrich M-7522], 1/100 protease inhibitor cocktail, in double distilled water) in a 1:1 (v/v) ratio and incubated at room temperature (RT) for 10 mins. The protein sample was loaded into an acrylamide gel (30% Acrylamide/Bis Solution, 29:1 [Bio Rad, Cat#: 161-0156], 0.5 M Tris-HCl pH 6.8, 20% SDS, 0.1% TEMED Omnipur [Calbiochem 8920], and 10% APS) and a 25 milliamps/gel current was applied for 75 mins. Protein was then transferred onto an Immobilon PVDF membrane (Cat. No. IPVH00010) pre-wetted with methanol at 100 V for 1 hr at RT. Membranes were then blocked with 5% milk in Tris-Buffered Saline and Tween 20 (TBST) for 1-2 hrs at RT to reduce non-specific binding. Membranes were then probed with primary antibody diluted 1/1000 in TBST with 5% milk overnight at 4°C then washed with fresh TBST 3 times for 10 mins each at RT. Secondary antibody conjugated to horseradish peroxidase (HRP) was then diluted 1/5000 in TBST with 5% milk and added to membranes for 2 hrs at RT. Membranes were again washed with fresh TBST 3 times for 10 mins each at RT. Enhanced chemiluminescence (ECL) (Western blotting reagents, GE Healthcare 45000875) was then added to membranes for 3-5 mins or with Enhanced Peroxidase Chemiluminescent Substrate (Cytodiagnostics, SR-04-04) for 1-3 mins. The Carestream Molecular Imaging station was used to visualize membranes. For re-probing, membranes were washed with double distilled water for 5 mins then the antibody was stripped with 0.2 M NaOH for 10 mins and membranes washed again with double distilled water for 5 mins. Semiquantification of the relative band intensity was done using Image J software. The same protocol was used for immunoblotting kidney tissue with the exception of the first washing steps with 1x PBS.

2.5 Immunofluorescence on tissue: For formalin fixed, paraffin embedded tissue, sections were first placed in xylene overnight at RT to remove paraffin. Sections were then washed 3 times in 100% ethanol for 10 mins each, in 95% ethanol 2 times for 10 mins each, in 75% ethanol once for 10 mins, then rinsed in double distilled water. For target retrieval, slides were placed in boiling TEG buffer (10 mM Tris Base, 0.5 mM EGTA, pH: 9) for 16 mins and let to cool for 1-2 hrs. Sections were then placed in 50 mM ammonium chloride (NH_4Cl) in 1x PBS for 30 mins. For blocking, the sections were placed in blocking buffer containing 1% BSA, 0.2% gelatine, and 0.05% saponin in 1x PBS 3 times for 10 mins each at RT. New blocking buffer was added for every incubation period. Primary antibody diluted 1/50 in 0.1% BSA, 0.3% TritonX-100 in 1x PBS was added to the sections, and placed in a humidity chamber overnight at 4°C. Sections were then warmed to RT before washing with 0.1% BSA, 0.2% gelatine, 0.05% saponin in 1x PBS solution 3 times for 10 mins each. Secondary antibody diluted 1/100 in 0.1% BSA, 0.3% TritonX-100 in 1x PBS was added to the sections and placed in a humidity chamber for 1 hr at RT. Sections were then rinsed in 1x PBS 3 times for 10 mins each, once in double distilled water and a coverslip mounted with DAKO.

2.6 Immunofluorescence on cells: NRK cells were grown to confluence in 12-well plates. Cells were first washed three times with cold 1x PBS with 1 mM $CaCl_2$ and 1 mM $MgCl_2$, pH 7.4. Cells were fixed using 4% paraformaldehyde for 20 mins on ice. 5% glycine in 1x PBS was used to quench fixation by washing three times. Cells were then blocked with 5% milk in 1x PBS at RT for 1 hr while rotating. TritonX-100 was added to blocking solution at a final concentration of 0.2% to permeabilize the membrane. Blocking solution was then aspirated and

fresh solution was added containing the indicated primary antibody at a 1/1000 dilution. Cells were incubated in primary antibody for 1 hr, gently shaking at RT. Cells were then washed three times with 1x PBS and fresh solution was added containing the indicated secondary antibody at a 1/1000 dilution. Again cells were incubated for 1 hr with gentle shaking at RT. After a final wash three times with 1x PBS cells were mounted on a microscope coverslip with DAKO and visualized under the microscope 24 hrs after mounting.

2.7 Cell Surface Biotinylation: This experiment uses biotin, a membrane impermeable chemical which covalently binds to lysine residues of cell surface expressed proteins. All buffers were cooled on ice prior to experimentation. Confluent cells were first placed on ice and washed three times with 1x PBS, pH 7.4. 1 mg/ml EZ-Link Sulfo-NHS-SS-biotin (Cat#: 21331, Thermo) in 1x PBS was added to the cells and incubated on ice twice for 15 min each with gentle shaking. After incubation with biotin, cells were washed three times for 10 min each with 5% (w/v) glycine in 1x PBS for quenching and rinsed five times with 1x PBS. Cells were then lysed with RIPA buffer containing 1/100 of proteinase inhibitor and phenylmethane sulfonyl fluoride (PMSF), adjusted to pH 7.4), scrapped and homogenized as described above. After 30 min incubation on ice, cells were centrifuged at 12,000 RPM at 4°C for 20 min. The supernatant was collected in a new tube. A 15 µl aliquot was taken for the total cell fraction control. The remaining sample was then incubated with streptavidin beads in a 1:2.5 (v/v) ratio for 1 hr rotating at 4°C. The beads attached to biotin are collected in a pellet fraction after 30 sec centrifugation at 14,000 RPM at 4°C and 15 µl of the supernatant collected for the post-streptavidin control fraction. The pellet fraction was then washed three times with 500 µl fresh RIPA buffer and centrifuged. The total cell lysate, streptavidin bound fraction and the post-

streptavidin control were then incubated in Laemmli buffer for 15 min before undergoing SDS-PAGE as described above.

2.8 Measurement of sodium/proton exchange activity: Low passage cells (<10) were grown in a 24 well plate seeded at a density of 100,000 cells/well on glass coverslips 24 hrs before the experiment. Cells were grown to 100% confluency prior to experimentation. Cells were first washed 2-3 times with Iso Na^+ (140 mM NaCl, 3 mM KCl, 1 mM $MgCl_2$, 1 mM $CaCl_2$, 20 mM Hepes, 10 mM D-glucose, adjusted to pH 7.4 with Tris Base). 5 mM BCECF-AM was then added, and cells incubated in a non-CO_2 incubator for 15-30 min at 37°C. Coverslips were then mounted into a cuvette using a holding device as described elsewhere (Krishnan *et al.,* 2015). Cells were next exposed to a dual wavelength excitation (440 and 490 nm) and emitted light captured at a 530 nm wavelength. Cells were perfused with Iso Na^+ for 5 mins before addition of 10 mM NH_4Cl for a further 5 mins to increase intracellular pH. Perfusion was then switched to Iso K^+ (140 mM KCl, 1 mM $MgCl_2$, 1 mM $CaCl_2$, 20 mM Hepes, 10 mM D-glucose, adjusted to pH 7.4 with Tris Base) for 3 mins causing rapid intracellular acidification. Perfusion was next switched back to Iso Na^+ to induce sodium-dependant pH recovery. If sodium/proton exchangers are expressed on the cell surface, they will catalyze the isoelectric exchange of extracellular sodium for intracellular protons thereby increasing intracellular pH to near basal levels. Calibration was performed using Iso K^+ of varying pH in the presence of 10 μM nigericin, a potassium/proton ionophore (Cat#: N7143, Sigma). After determining the 490/440 ratio intensity at a known pH, intracellular pH was calculated from the calibration curve. This protocol was optimized for use on NRK cells, but for AP-1 cells, a sodium-free buffer (140 mM *N* methyl-D-glucamine [NMDG], 3 mM KCl, 1 mM $MgCl_2$, 1 mM $CaCl_2$, 20 mM Hepes, adjusted

to pH 7.4 with Tris Base) was used instead of Iso K^+ and 50 mM NH_4Cl was used instead of 10 mM NH_4Cl in order to alkalize the cells.

2.9 Transepithelial calcium-45 flux assay: This protocol was modified from Pan and colleagues (Pan *et al.,* 2012). Cells were plated in a 24 well plate on a transwell permeable support (Corning) at a concentration of $4.4x10^3$ cells per 250 µL media. Cells were grown for 5 days in order to form monolayers. Both apical and basolateral surfaces of the cells were first washed three times with Radiation (RA) buffer (140 mM NaCl, 3 mM KCl, 1 mM $MgCl_2$, 1 mM $CaCl_2$, 10 mM Hepes, 10 mM D-glucose, adjusted to pH 7.4 with Tris Base) without radionuclide and incubated in a non-CO_2 incubator at 37°C for 10 mins. During this incubation period, either vehicle or 100 µM EIPA was added. The apical buffer was then aspirated and 250 µL RA buffer with 25 µCi/ml $^{45}Ca^{2+}$ was added. 10 µL aliquots were taken from the basolateral side at times 0, 5, 10, 14, 18, 22, 26, and 30 mins as well as the total radiation in order to calculate calcium flux (J_{Ca}^{++}) in mmol/h•cm^2.

2.10 Calcium-45 uptake assay: Low passage (<10) NRK cells were seeded at a density of 60,000 cells per well in a 24 well pate 48 hrs before experimentation to allow cells to reach confluency. Media was changed 1 hr before the experiment and then washed with 250 µl phosphate-free KHB buffer (140 mM NaCl, 3 mM KCl, 1 mM $MgCl_2$, 1 mM $CaCl_2$, 20 mM Hepes, 20 mM Na-acetate, 10 mM D-glucose, 4 mM L-Lactate, 1 mM L-Alanine, adjusted to pH 7.4 with Tris Base) three times. Cells were then incubated in 500 µl phosphate-free KHB buffer for 10 min in a 37°C non-CO_2 incubator. The entire plate was then emptied at once by inversion into paper towel. 500 µl uptake buffer (KHB, 2 mM NaH_2PO_4, 10 µM Felodipine, 10 µM

Verapamil, and 10 μCi/ml $^{45}Ca^{2+}$) was added to each well. Depending on the protocol, cells were either incubated with uptake buffer over time (1, 5, 10, 20, 40, and 60 min), incubated for 5 min in the presence of increasing extracellular $CaCl_2$ concentration or incubated for 5 min in the presence of increasing extracellular proton concentration. Cells were then washed 5 times with 250 μl ice-cold stop buffer (KHB with 1.5 mM $LaCl_3$) to quench the uptake and wash excess calcium off the cell surface. Cells were then lysed with 0.1% sodium dodecyl sulfate, incubated for 10 min at RT while shaking and lysate was taken to the multipurpose scintillation counter.

2.11 Ratiometric calcium imaging: This protocol was developed for measuring the rate of calcium uptake using FURA-2, a ratiometric dye, in Normal Rat Kidney (NRK) cells and is a modified version from Miederer and colleagues (Miederer *et al.,* 2014). NRK cells were plated in 6 well plates on glass coverslips (Fisher brand microscope cover glass 12-5451-102 25CIR-1). Cells were seeded at a concentration of 500,000 cells per well in 2 ml of media and grown for 48 hrs prior to experimentation to ensure the cells were confluent. Only cells of low passage (<10) were used for calcium imaging. The coverslips with cells were transferred into a 10 mm culture dish and 2 ml media/buffer was added. Cells were washed 3 times with 0.5 mM $CaCl_2$ Ringer's solution (140 mM NaCl, 3 mM KCl, 1 mM $MgCl_2$, 0.5 mM $CaCl_2$, 5 mM Hepes, 10 mM D-glucose, adjusted to pH 7.4 with Tris Base) then loaded with 1 μM of the calcium sensitive dye FURA-2, AM purchased from Molecular Probes (F1221) dissolved in DMSO with 0.1% Pluronic F-125 solution (Molecular Probes, P-1572) and swirled until dissolved. Concurrently, 2 mM Probenecid dissolved in NaOH (Sigma-Aldrich P-8761) was added to inhibit efflux of the dye. Cells were incubated at room temperature for 2 hrs with gentle shaking in the dark. Cells were visualized using a Leica DMI6000B microscope with a Lambda DG4P-215 lamp supply,

and Quorum MAC6000 modular automation controller system. Cells were excited at 340 nm and 380 nm wavelengths, and emitted light at 530 nm and captured using a Hamamatso Orca-Flash 4.0 digital camera (C11440). MetaFluor Fluorescence ratio imaging software was used for collecting the data. The microscope stage, objective lens, and buffers were held at 37°C for the duration of the experiment. Cells were first perfused with a 0.5 mM $CaCl_2$ Ringer's solution for 5 min. The solution was then switched to the same Ringer's solution but instead containing 1.5 mM $CaCl_2$ for 10 min to prime the cells. The solution was then switched to a $CaCl_2$ free Ringer's solution for 10 min then the 0.5 mM solution was added back to measure calcium uptake. Pharmaceuticals were added during this final uptake phase i.e. either: 5-(*N*-Ethyl-*N*-isopropyl) amiloride, EIPA (Sigma-Aldrich A3085-25 mg), Verapamil (Sigma-Aldrich V4629), Lanthanum chloride heptahydrate (Fisher Scientific L9-50) or Ruthenium Red (Sigma-Aldrich R275-1). Two measurements were taken during uptake: the maximal amount of calcium taken up and the slope of the initial 15 sec after switching back to a calcium containing solution. To convert the 380/340 nm ratio into intracellular calcium concentration, three calibration buffers were used to measure the minimum ratio (0 mM $CaCl_2$), the maximum ratio (10 mM $CaCl_2$) and one for quenching the fluorescence of FURA-2 to measure the background fluorescence (2 mM $MnCl_2$). The calcium ionophore Ionomycin (Sigma I9657) was added to each calibration buffer. Using the conversion equation derived by Grynkiewicz and colleagues (Grynkiewicz *et al.,* 1985), the ratio measured was converted to concentration of intracellular calcium $[Ca^{2+}]_i = Kd * ((R-R_{min}) / (R_{max}-R)) * (Sf_2/Sb_2)$ where the dissociation constant of FURA-2 was determined as 225 nM for intracellular conditions, R is the measured ratio, R_{min} is the ratio at 0 mM calcium, R_{max} is the ratio at 10 mM calcium, Sf_2 is the fluorescence intensity of 380 nm excitation at 0 mM calcium and Sb_2 is the fluorescence intensity of 380 nm excitation at 10 mM calcium.

2.12 RNA interference: NHE8 siRNA (s161363 & s161361 ambion by life technologies, Silencer ® Select Pre-designed [Non-inventoried] siRNA, 01136966) was diluted 1/10 in Opti-MEM I (1x) Reduced Serum Medium (Cat#: 31985-070, Gibco by life technologies) and mixed gently by pipetting. Oligofectamine (Cat#: 12252011 Thermo Fisher) was diluted 1/100 in Opti-MEM and mixed gently by pipetting. Both solutions were incubated for 15 min at RT. After incubation, the oligofectamine and siRNA were combined in a 1:1 (v/v) ratio and incubated for a further 15 min at RT. NRK cells were first washed with 1x PBS and trypsinized for 15 min at 37°C in a 5% CO_2, 95% air incubator. Cells were collected in a 50 ml tube using 10 ml DMEM and centrifuged at 1500 RPM for 5 min. Cells were resuspend in 10 ml Opti-MEM and 10 µl taken for counting. Opti-MEM was added to the desired concentration. Cells were added to the oligofectamine and siRNA mixture to a final volume of 500 µl and then plated. Cells were incubated at 37°C in a CO_2 incubator for 4 hrs after which the media was replaced with 500 µl DMEM supplemented with 30% FBS. Assays for gene/protein expression were conducted at time 24, 48 and 72 hrs. For the 48 and 72 h incubations, an additional transfection was done at 24 hrs (double transfection). Low passage cells (<10) were used for RNA interference. Cells were counted using a haemocytometer and plated at a density of 100,000 cells/500 µL/well in 24-well plates (Thermo Fisher Scientific, 75 Panorama Creek Drive, Rochester, NY 14625-2385, BioLite 6 well multidish 130184). The final siRNA concentration was 100 nM and the final concentration of oligofectamine 8 µg/ml according to the manufactures protocol. Ultimately this resulted in incomplete knockdown that was highly variable.

CHAPTER 3: RESULTS

3.1 Renal NHE8 mRNA levels are reduced and protein levels increased in cinacalcet and vitamin D treated mice: The Alexander lab performed an mRNA microarray analysis to identify novel mediators of calcium homeostasis. To this end, the renal expression of genes from mice that were treated with the CaSR agonist cinacalcet or with vehicle was examined. Experimental details of these studies can be found in Dimke *et al.,* 2013 (Dimke *et al.,* 2013). The results from the microarray revealed a nearly 50% reduction of NHE8 mRNA expression in cinacalcet treated mice compared to vehicle controls (Alexander lab unpublished data). In order to confirm these results, we used quantitative real time PCR analysis (qPCR) of NHE8 from the same kidney samples and similarly observed a 50% reduction in NHE8 mRNA levels in cinacalcet treated mice compared to vehicle controls **(Figure 2A)**. In contrast, when analyzing the protein expression from lysate generated from the same kidneys, NHE8 was significantly increased by nearly 40% in the cinacalcet treated group **(Figure 2 D&E)**. Wild-type FVN mice were also treated with active vitamin D and both gene and protein expression of NHE8 determined. qPCR was used to determine the change in renal NHE8 mRNA expression in vitamin D treated mice compared with vehicle controls. Similar to cinacalcet treated mice, NHE8 mRNA was significantly reduced by nearly 40% **(Figure 2B)** however there was a slight but significant increase in NHE8 protein expression in the vitamin D treated verses control groups **(Figure 2 F&G)**. Lastly, qPCR was performed on kidney from mice fed a high (2%), normal (0.6%) or low calcium diet (0.01%) for NHE8 mRNA levels (Dimke *et al.,* 2013). There was no significant difference between the groups or between 10 and 21 day treatments **(Figure 2C)**. Together our findings infer that renal NHE8 expression is altered by perturbations to calcium homeostasis.

3.2 NHE8 localizes to the apical brush border membrane of mouse proximal tubules: To determine the cellular localization of NHE8 in proximal tubules, kidneys from wild-type mice

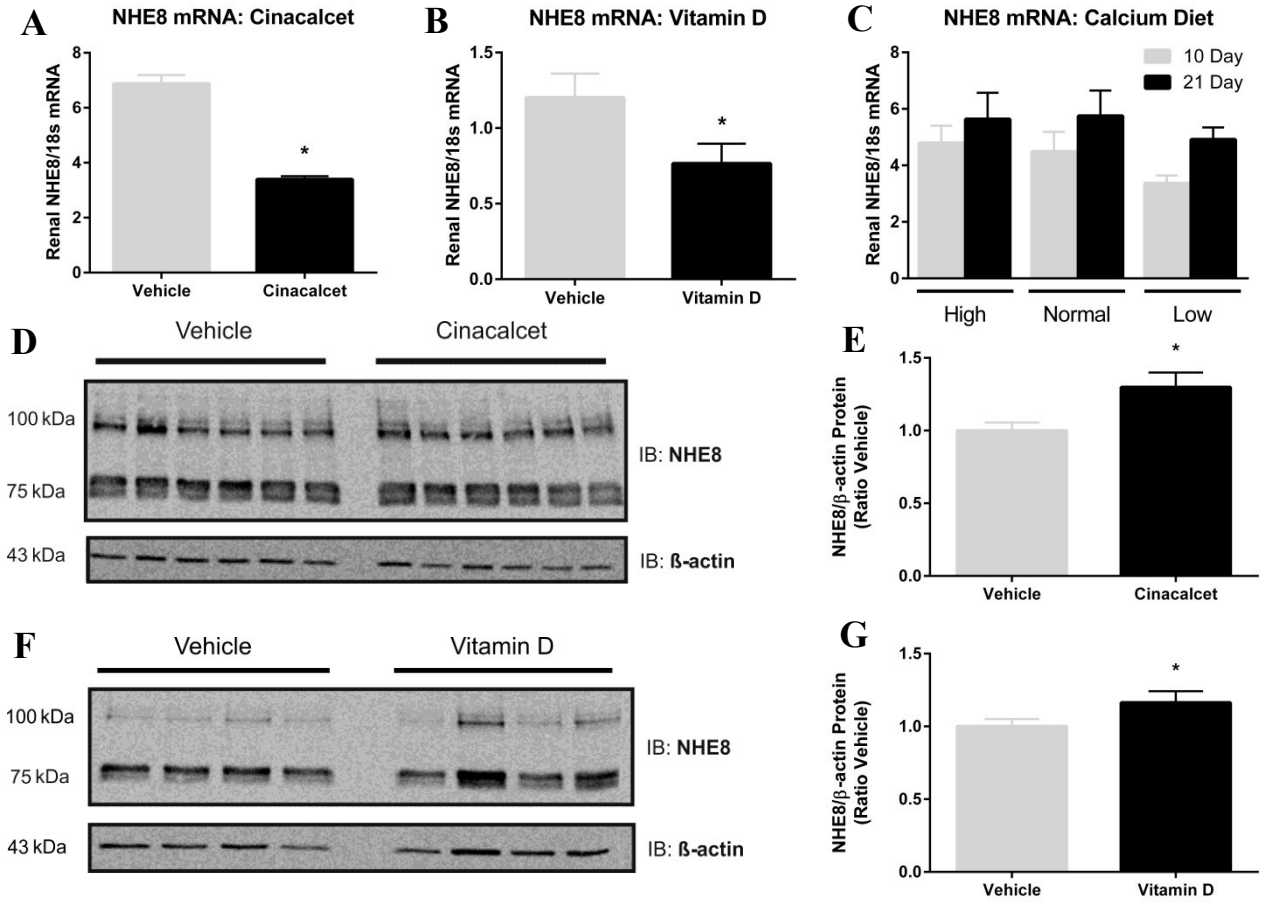

Figure 2) Renal NHE8 mRNA levels are reduced and protein levels increased in cinacalcet and vitamin D treated mice: Quantitative real time PCR and Western Blot analysis of mouse renal NHE8 expression. The Alexander lab performed a microarray on mRNA isolated from the kidney of mice treated with the calcium sensing receptor agonist cinacalcet (unpublished). This revealed that the sodium/hydrogen exchanger isoform 8 (NHE8) mRNA expression was decreased. Quantitative real-time PCR (qPCR) analysis of NHE8 mRNA expression was used to confirm these findings for mice treated with cinacalcet (A). N=6 for each group. Further, qPCR was used to determine NHE8 mRNA expression in kidney from mice treated with vitamin D (B). N=8 for each group. NHE8 mRNA expression was also analyzed by qPCR in kidney from mice fed different calcium containing diets for either 10 or 21 days (C). N=8 for each group. For A, B, and C, NHE8 is normalized to 18S ribosomal RNA. Kidney lysate from the same mice treated with cinacalcet (D) or vitamin D (F) were immunoblotted with mouse anti-NHE8 antibody (7A11). NHE8 protein abundance was normalized to β-actin for each mouse and results are graphed as a ratio normalized to vehicle. Panel (E) and (G) show immunoblot semi quantification for (D) and (F) respectively. Data are displayed as mean ± S.E *P<0.05.

fed a normal calcium containing diet were isolated and then immunostained with rabbit anti-NHE8 (Cy3) and the nucleus in DAPI. Sections were also probed with Lotus tetragonolobus lectin, a specific mouse proximal tubule brush border membrane marker, shown in green. Images were taken of the cortex which primarily contains proximal tubule (>80%) cells **(Figure 3 A&B)**. NHE8 colocalizes with the proximal tubule marker confirming that it is expressed in the apical brush border membrane of proximal tubule cells. These sections were also stained with a mouse anti-NHE8 monoclonal antibody (7A11), which does not bind to protein in kidney sections **(Figure 3 A&C)**. Images were also taken without the addition of primary antibody in order to analyze the amount of background staining with the secondary antibody Cy3 (see appendix). Images were taken near the centre of the kidney section known as the medulla **(Figure 3 C&D)**. This area of the kidney does not contain proximal tubule cells and NHE8 was not detectable there. This confirms that NHE8 is present in the apical brush border membrane of mouse kidney as has been previously reported (Goyal *et al.,* 2005).

3.3 NHE8 localizes to the apical membrane in NRK cells: In order to examine the potential role of NHE8 in renal proximal tubular calcium handling, we sought a cell culture model. Normal rat kidney cells have been used to this end previously (Zhang *et al.,* 2007). NRK cells were therefore grown to confluence and visualized using confocal microscopy. Cells were probed with mouse anti-NHE8 antibody (7A11) and with anti-ZO-1 antibody to identify the apical tight junctions (Schnittler 1998) **(Figure 4A)**. XZ images show ZO-1 in the apical membrane at cell to cell contacts. NHE8 localizes to the apical membrane as is evident in the merged image. In addition, cell surface biotinylation experiments on confluent NRK cells demonstrate NHE8 protein expression in the apical membrane but not the intracellular control, β-actin **(Figure 4B)**. The mouse anti-NHE8 antibody binding specificity is demonstrated by its

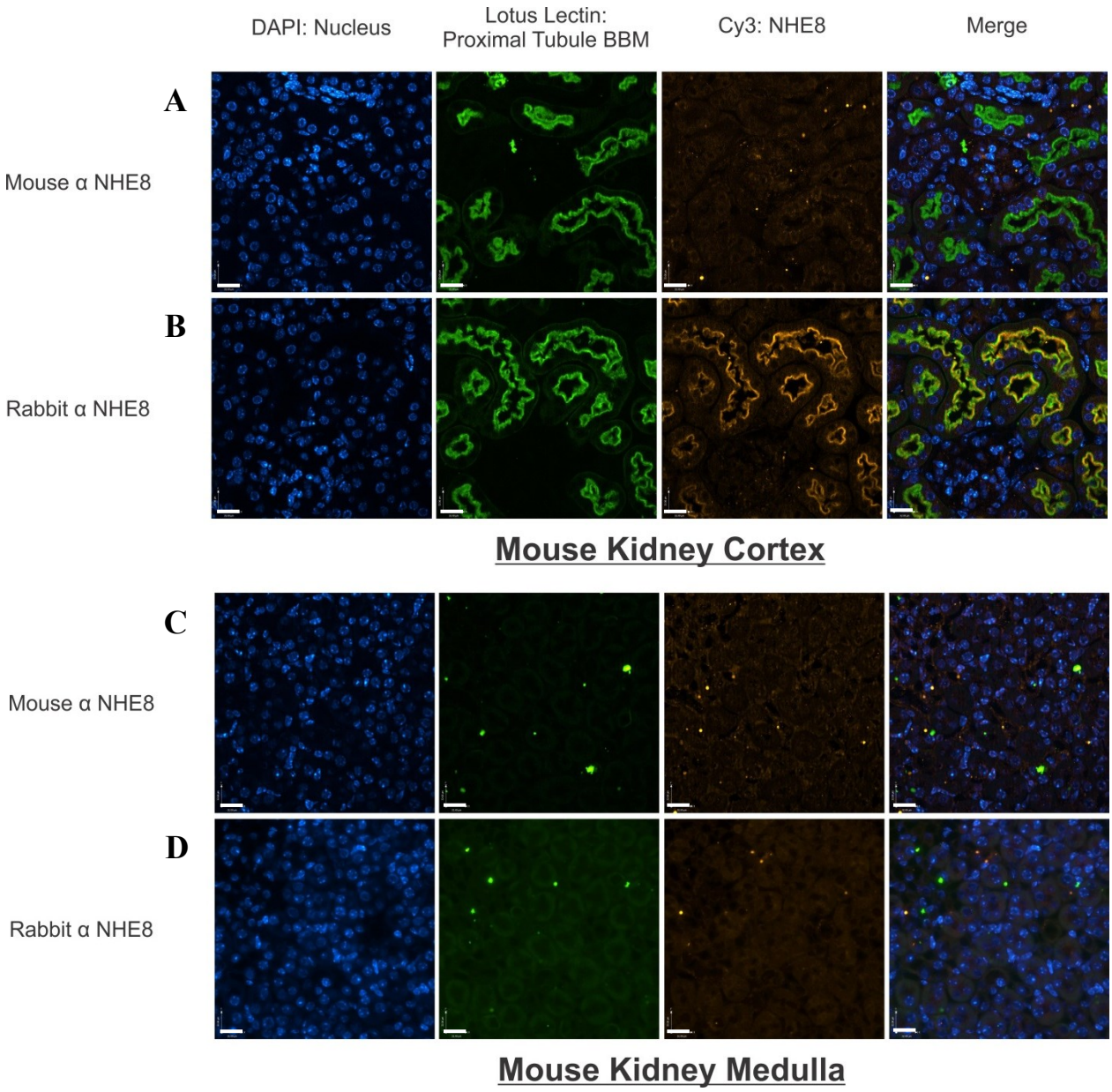

Figure 3) NHE8 localizes to the apical brush border membrane of mouse proximal tubules: Kidney sections were prepared from wild-type FVB mice and protein expression analyzed using immunofluorescence microscopy. Images of the mouse kidney cortex were taken in panel (A, B) and of the medulla in panel (C, D). Two primary antibodies were used to detect NHE8: a monoclonal mouse-derived antibody (7A11) (A, C) and a rabbit-derived polyclonal (B, D). The nucleus is stained with 4,5-diamidino-2-phenylindole (DAPI), NHE8 in Cy3 and lotus lectin in green marking the proximal tubule brush border membrane. Merged images show regions of co-localization in olive brown. White bars indicate a 32 μm scale.

ability to detect NHE8 in mouse kidney lysate and in NRK cells which is attenuated when NRK cells are treated with NHE8 siRNA **(Figure 4C)**. The confluency of NRK cells also changes NHE8 expression as revealed by immunoblot analysis **(Figure 4D)**. Lysate was collected from cells at different percentage confluence (10% to 100%) and subjected to SDS-PAGE. As the cells become increasingly confluent, NHE8 is expressed more at the higher molecular weight and less at the lower molecular weight band. The quantity of protein loaded was not different between samples as is evident by an equal amount of the loading control β-actin being present in the same blot after stripping and reprobing. These results demonstrate apical expression of NHE8 in NRK cells.

3.4 Treatment with 1 μM EIPA diminishes NHE activity in NRK cells but 10 μM EIPA is required to reduce NHE1 activity in AP-1 cells: To assess NHE functional activity in NRK cells, we used a sodium-dependent pH recovery assay. Using the ratiometric fluorescent and pH sensitive dye BCECF AM, we determined that 100 nM EIPA inhibits 50% of NHE activity in NRK cells whereas there is complete loss of NHE activity in the presence of 1 μM EIPA **(Figure 5 A&B)**. To determine the concentration of EIPA required to inhibit NHE1 which is also expressed in NRK cells (Zhang *et al.,* 2007), the same experiment was performed on AP-1 cells over-expressing NHE1 **(Figure 5 C&D)**. 100 nM EIPA did not have a significant effect on sodium-dependent pH recovery whereas 1 μM EIPA reduced activity by 45% and 10 μM EIPA treatment resulted in complete loss of activity. Sodium-dependent pH recovery was determined as the change in intracellular pH over the first 100 sec of pH recovery after re-addition of extracellular sodium. Therefore we can conclude that 1 μM EIPA completely abolishes NHE8 activity in NRK cells, and there is little residual NHE1 activity.

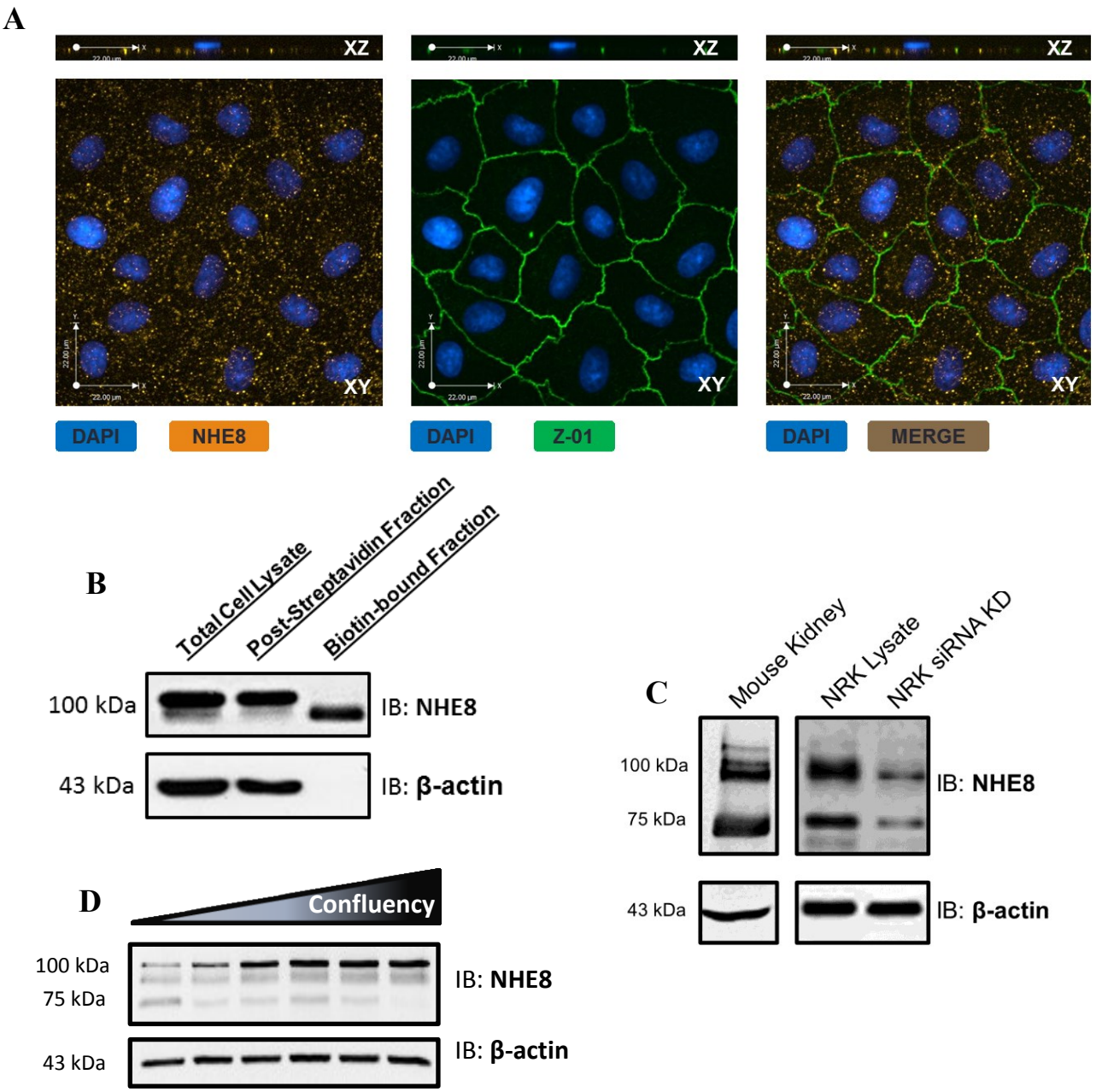

Figure 4) NHE8 localizes to the apical membrane in NRK cells: Apical expression of NHE8 was demonstrated using immunofluorescence confocal microscopy (A) and cell surface biotinylation analysis (B). XY and XZ confocal image of confluent NRK cells were immunostained with anti-NHE8 (Cy3), DAPI, and the apical tight junction marker ZO-1 in green (A). XZ image shows the apical membrane below the cells and the basolateral above and beside. Panel (C) demonstrates NHE8 antibody (7A11) binding specificity on immunoblots of mouse kidney and NRK cells with and without NHE8 siRNA treatment. (D) NRK cell lysate was collected at 6 time points of increasing confluency and immunoblotted with anti-NHE8. Membranes were stripped and re-probed for β-actin to ensure consistent loading.

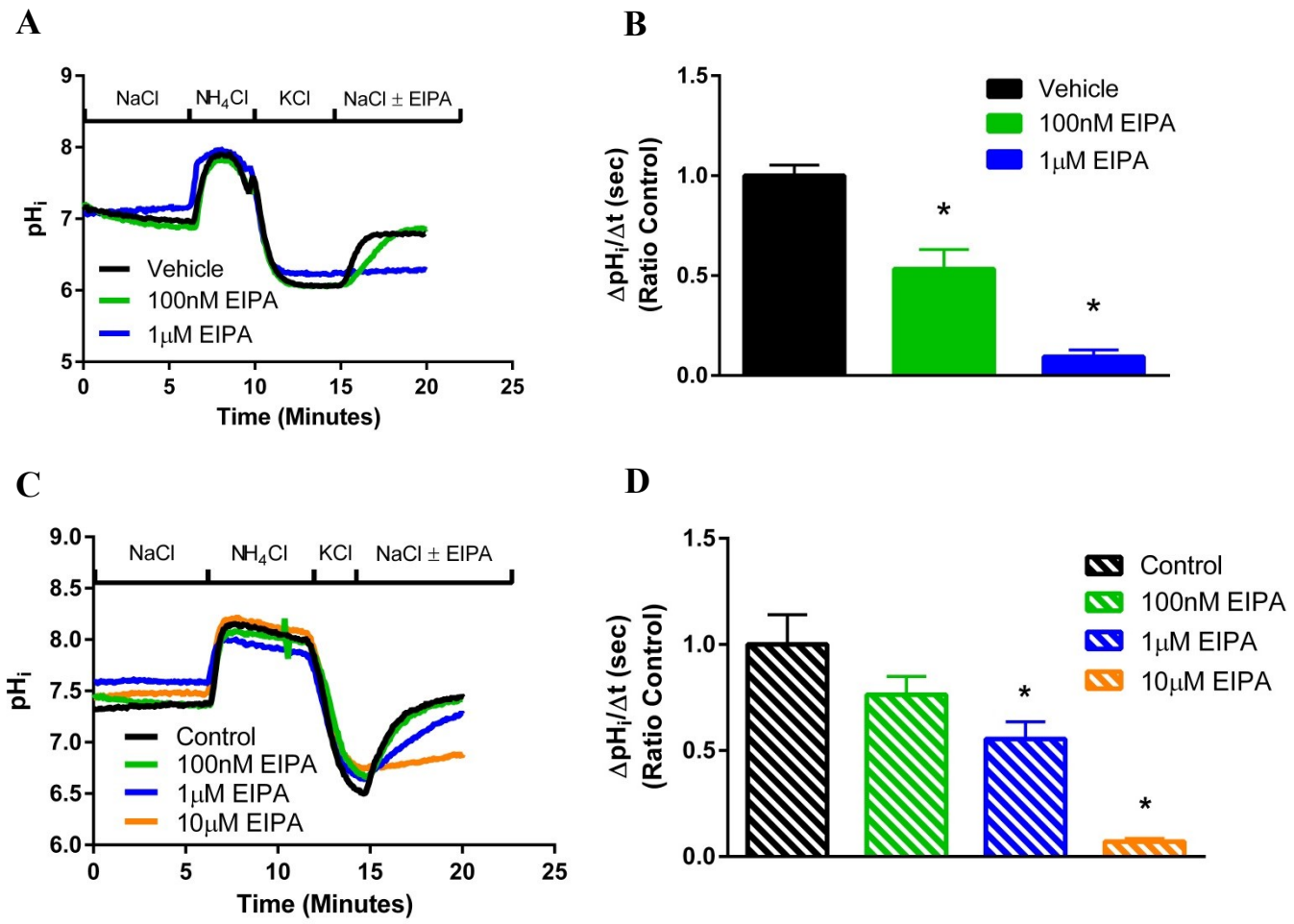

Figure 5) Treatment of 1 μM EIPA diminishes NHE activity in NRK cells however 10 μM EIPA is required to reduce NHE activity in AP-1 cells: Sodium-dependent pH recovery was assessed in NRK cells (A, B) and AP-1 cells (C, D) with varying concentrations of EIPA. Cells were first perfused with sodium-containing Ringer's buffer and then alkalized by addition of NH_4Cl. Washing the cells in a sodium and ammonium free Ringer's solution caused cell acidification. Representative traces of the change in pH_i after re-addition of sodium-containing Ringer's buffer for NRK cells (A) and AP-1 cells expressing NHE1 (C). The rate of recovery was calculated as the change in pH over the change in time during the first 100 sec of recovery in NRK cells (B) and AP-1 cells (D). N=6 for each group. Data are displayed as mean ± S.E *P<0.05.

3.5 Transepithelial calcium flux is not affected by NHE inhibition in NRK cells: To examine the role of NHE8 in transepithelial calcium flux, we measured the rate of calcium-45 appearance in the basolateral media after apical addition to confluent monolayers of NRK cells over a 30 min time interval in the presence and absence of EIPA. NRK cells were grown to confluence on semipermeable filters separating apical from basolateral solutions. There was no difference in calcium-45 flux between vehicle and 100 μM EIPA treated cells **(Figure 6 A&B)**. Calcium-45 flux was measured as nmol calcium per hr per cell surface area. Importantly, in a loose epithelial model such as NRK cells, this assay primarily measures paracellular flux. Thus, inhibition of NHE8 activity does not alter paracellular flux across this proximal tubule cell culture model.

3.6 NHE activity in NRK cells does not affect uptake of calcium-45: To elucidate a role for NHE8 in calcium uptake into NRK cells, calcium-45 was added to confluent cells, allowed to incubate over time, uptake was then quenched with lanthanum (III) chloride, cells were washed, lysate collected and calcium-45 counted. Maximal calcium-45 uptake into NRK cells over time occurs at 5 to 10 mins. There was no difference between calcium uptake in vehicle or 1 μM EIPA treated cells over this time course **(Figure 7A)**. Further, examining calcium-45 uptake kinetics under increasing concentrations of extracellular calcium chloride revealed a Michaelis-Menten relationship where the R^2 for vehicle and EIPA were 0.92 and 0.95 respectively. There was no significant difference for the V_{max} or K_m between vehicle and 1 μM EIPA treated cells **(Figure 7B)**. Experiments investigating the effect of extracellular pH on calcium-45 uptake revealed an increased calcium-45 uptake at alkaline pH but no difference induced by treatment with EIPA **(Figure 7C)**. The effect of the calcium channel blockers verapamil and felodipine on

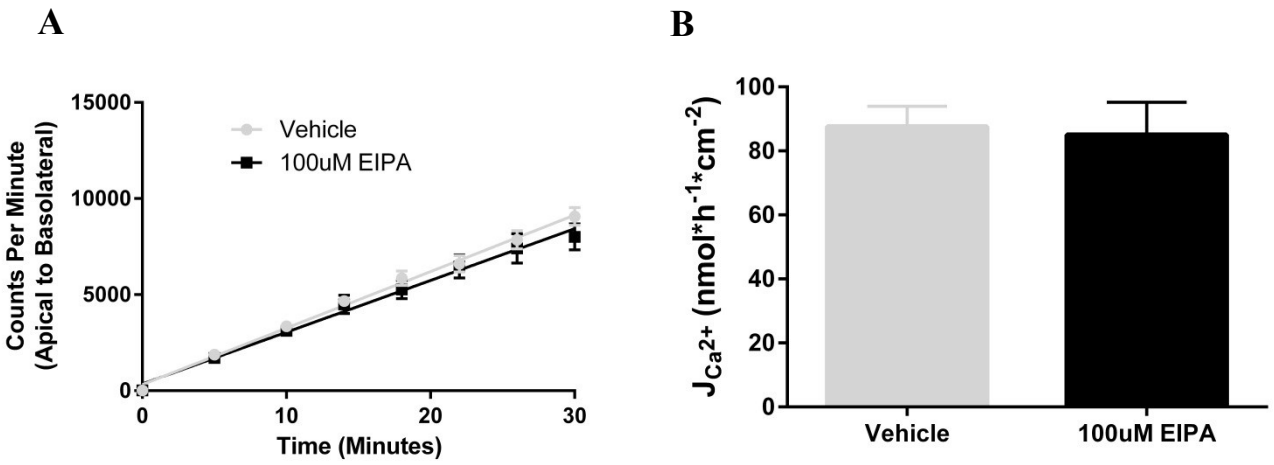

Figure 6) Transepithelial calcium flux is not affected by inhibition of NHE activity in NRK cells: Cells were grown on semipermeable filters where the apical and basolateral solutions are separated. Cell culture media was replaced with radiation buffer and cells were washed three times. Calcium-45 was added to the apical buffer and 10 µl basolateral samples were taken at the indicated times (A). The sample radioactivity was measured using a scintillation counter and calcium flux was calculated in the presence and absence of 100 µM EIPA added to both apical and basolateral solutions (B). N=6 for each group. Data are displayed as mean ± S.E.

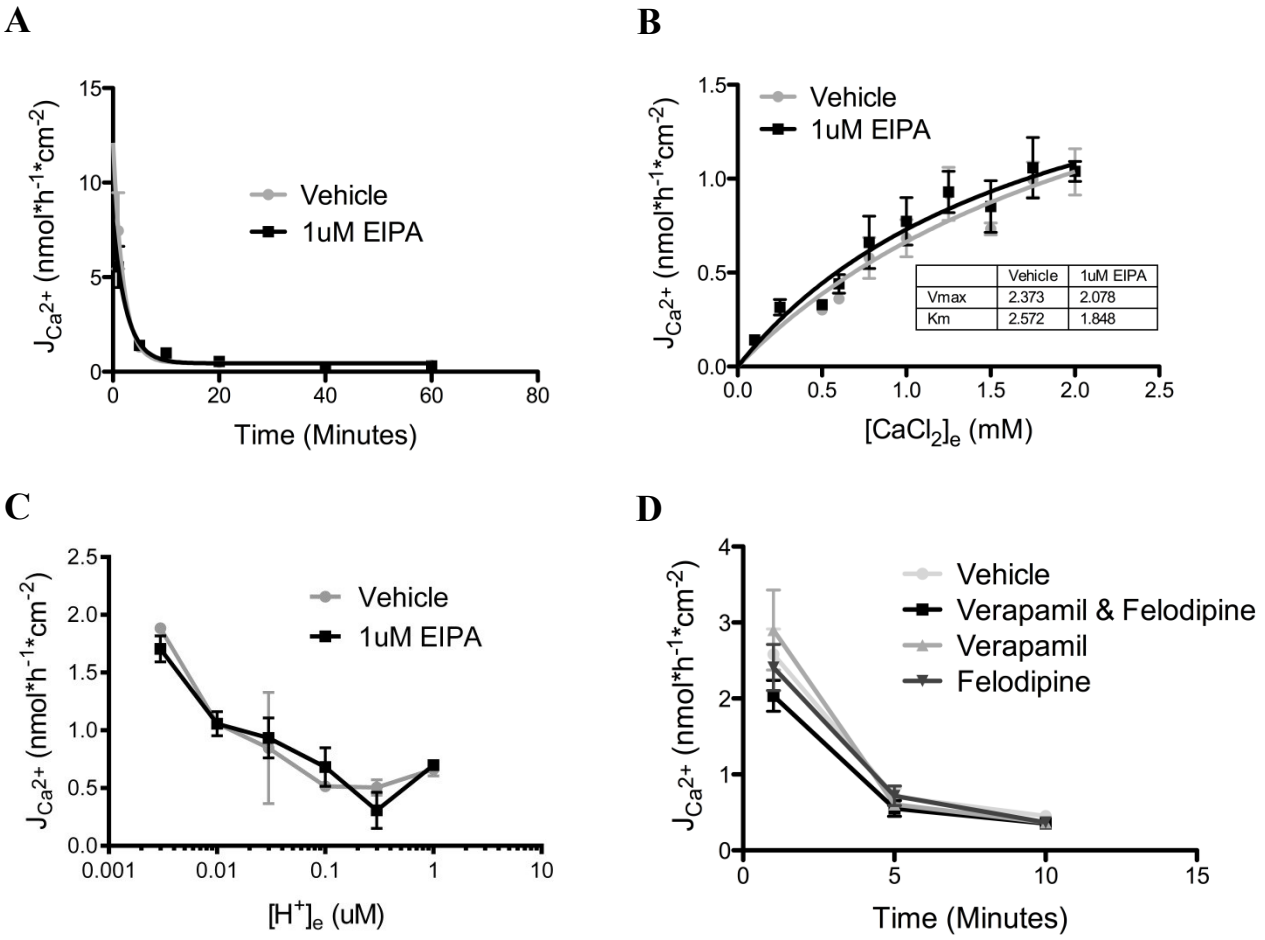

Figure 7) Calcium-45 uptake into NRK cells is not affected by inhibition of NHE activity: Confluent monolayers of NRK cells were incubated with calcium-45 under the given conditions, uptake was quenched using $LaCl_3$, and cell lysate analyzed. (A) Rate of calcium-45 uptake over time. N=6 for each group. (B) Calcium-45 flux at 5 min under varying calcium concentrations. Transport kinetic analysis is shown in the inset panel. N=9 for each group. (C) Calcium-45 uptake at varying extracellular pH; calcium-45 flux was calculated after 5 mins of uptake at each concentration of extracellular proton. N=3 for each group. (D) The rate of calcium-45 uptake in the presence and absence of calcium channel blockers. N=6 for each group. Each experiment was conducted in the presence of 10 μM Verapamil and Felodipine. Where indicated, calcium uptake was measured in the presence and absence of 1 μM EIPA. Data are displayed as mean ± S.E.

calcium-45 uptake between 1 and 10 min was also measured. There was no difference in calcium-45 uptake between vehicle and calcium channel blocker treated groups at any time point **(Figure 7D)**. Together these studies demonstrate that NHE8 activity inhibition does not alter steady state kinetics of calcium uptake into NRK cells. However, the sensitivity of these studies is such that initial calcium uptake into the cells could not be resolved.

3.7 Inhibition of NHE activity in NRK cells increases the initial rate of calcium uptake: In order to resolve the initial calcium uptake after NHE8 inhibition in NRK cells (i.e. the first 15 s) we used ratiometric imaging of intracellular calcium concentration with the calcium sensitive dye FURA-2 AM. Using this technique, two measurements were obtained: first, an assessment of total increase in intracellular calcium; what we refer to as the delta peak was taken. This is the measure of maximal calcium uptake after re-addition of extracellular calcium. Maximal calcium uptake occurred within the first 5 min of uptake consistent with our calcium-45 uptake data **(Figure 8A)**. Second, the initial change of intracellular calcium concentration over the first 15 sec of uptake was determined as a measure of initial calcium uptake **(Figure 8B)**. There was no difference in maximal calcium uptake between control and EIPA treated cells **(Figure 8C)**. There was, however, a nearly 1.5 fold increase in initial calcium uptake in the presence of 1 and 10 μM EIPA **(Figure 8D)**. Thus inhibition of NHE8 significantly enhances initial calcium uptake by NRK cells.

3.8 Calcium uptake in NRK cells is also enhanced by the absence of extracellular sodium, however sodium-dependent pH recovery is not altered in the absence of extracellular calcium: To further implicate NHE8 in initial calcium uptake, we replaced extracellular sodium with N-Methyl-D-glucamine, thereby eliminating cellular sodium/proton exchange activity **(Figure 9A)**. Under these conditions, the initial rate of calcium uptake was enhanced nearly 2-fold in the

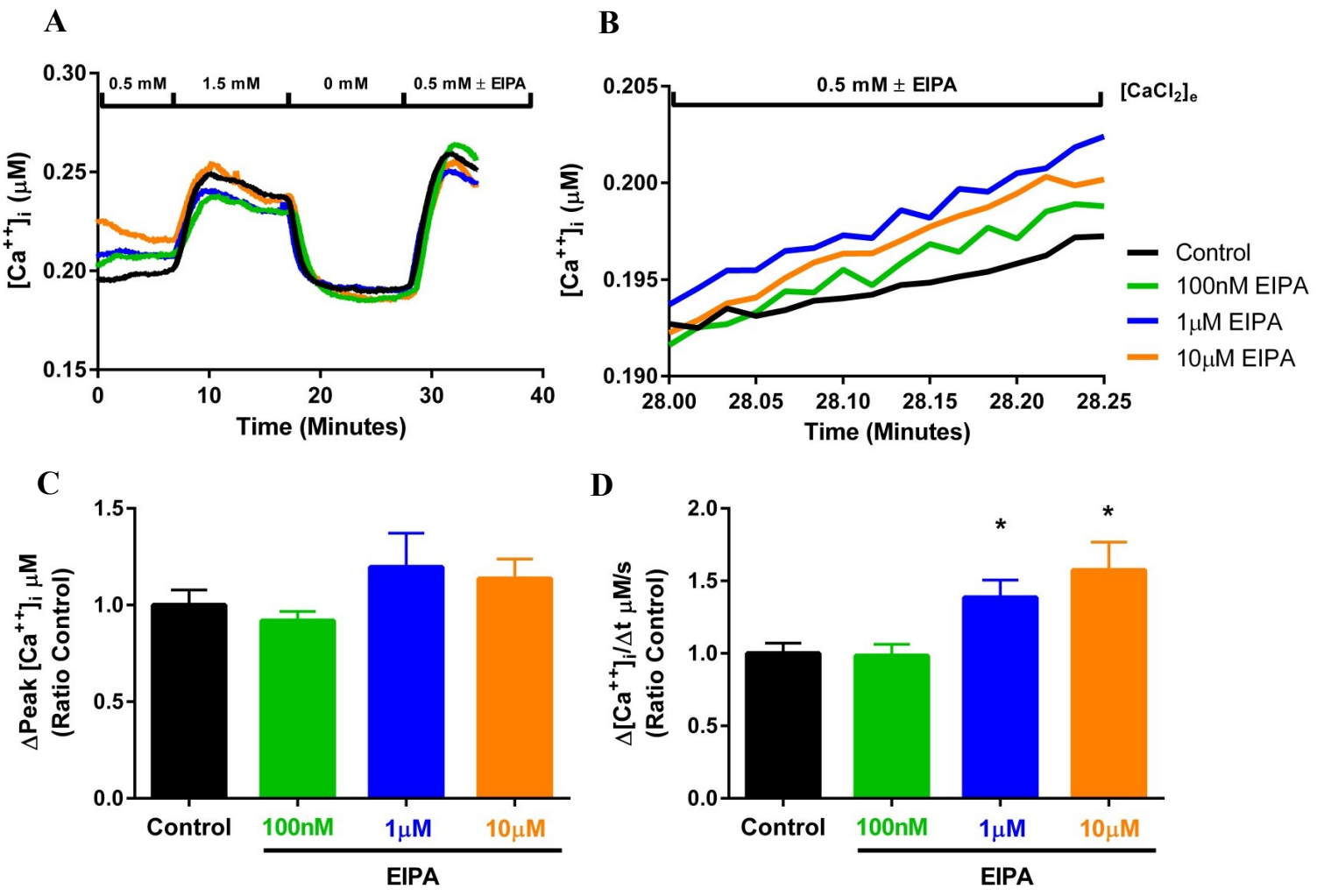

Figure 8) Inhibition of NHE activity in NRK cells increases the initial rate of calcium uptake: Calcium uptake was investigated in NRK cells using the calcium sensitive dye FURA-2 AM. Cells were perfused with 0.5 mM $CaCl_2$ until the intracellular calcium concentration was stable. The perfusate was then switched to a 1.5 mM $CaCl_2$ containing buffer as a pre-pulse. Next, buffer calcium concentration was dropped to a minimum using 0 mM $CaCl_2$ containing buffer in the presence of the calcium chelator EGTA. Once cells were at a minimum intracellular calcium concentration, uptake was measured after re-addition of 0.5 mM $CaCl_2$ (A-B). From the traces, two measurements were calculated: the change in peak from minimum extracellular calcium to maximum uptake after re-addition of 0.5 mM $CaCl_2$ (C) and the rate of calcium uptake during the first 15 sec of recovery (D). Varying concentrations of EIPA were added during the uptake period as indicated. The bar graphs represent the average of 6 independent experiments for the indicated conditions and an average of 20 individual cell recordings were calculated per experiment. The traces indicate representative measurements (A-B). Data are displayed as mean ± S.E *P<0.05.

absence of extracellular sodium **(Figure 9C)**. The maximal calcium uptake was also enhanced but not significantly **(P=0.06, Figure 9B)**. Further, we investigated NHE8 activity in NRK cells in the presence and absence of extracellular calcium during pH recovery **(Figure 9D)**. Under these conditions, NHE8 activity was not affected by removal of extracellular calcium **(Figure 9E)**. Thus, we again observed inhibition of NHE8 activity increasing calcium uptake into NRK cells, however removal of extracellular calcium does not affect sodium/proton exchange via NHE8.

3.9 Calcium uptake into NRK cells is mediated by calcium channels: To determine possible calcium entry mechanisms into NRK cells, we investigated changes in calcium uptake upon treatment with various calcium channel blockers **(Figure 10A)**. **Figure 10 B&C**: Lanthanum (III) chloride, a divalent cation channel blocker almost completely prevented calcium uptake compared with controls, however it did not significantly alter the rate of initial calcium uptake. Ruthenium red, a non-selective channel blocker, attenuated both maximal calcium uptake and the initial rate of calcium uptake by roughly 70%. Verapamil, a selective L-type calcium channel blocker, attenuated maximal calcium uptake by roughly 50% and initial uptake by roughly 40%. It therefore appears that calcium uptake into NRK cells is mediated by one or more calcium channels, the identity of which is completely unknown.

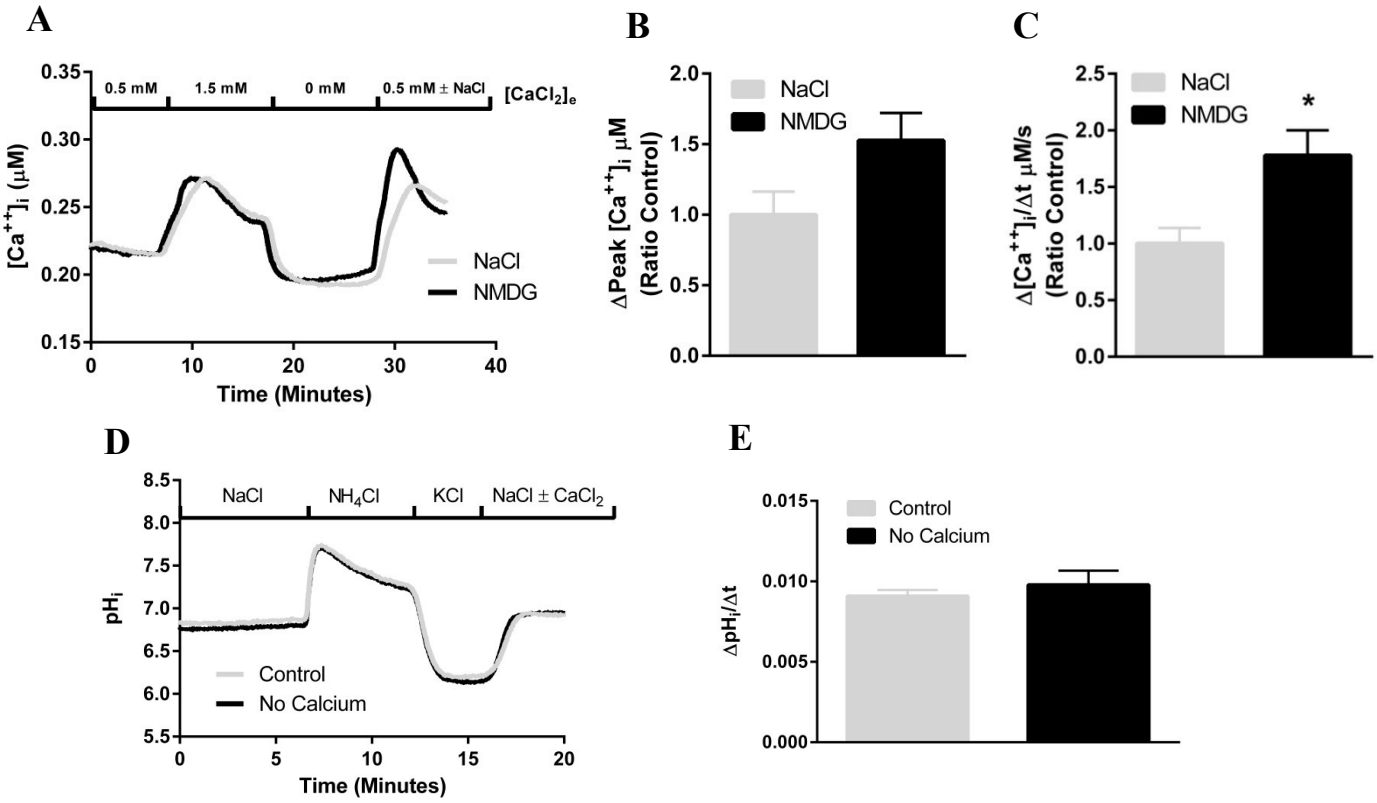

Figure 9) Calcium uptake in NRK cells is increased by the absence of extracellular sodium, however sodium-dependent pH recovery is not altered in the absence of extracellular calcium: Calcium uptake was investigated in NRK cells using the protocol described in **Figure 8** in the presence and absence of extracellular sodium (A). Sodium free buffer contained 140 mM N-Methyl-*D*-glucamine (NMDG) to replace 140 mM NaCl. Two measurements were determined: the change in peak from minimum extracellular calcium to maximum uptake after re-addition of 0.5 mM $CaCl_2$ (B) and the rate of calcium uptake during the first 15 sec of recovery (C). Sodium-dependent pH recovery was investigated in NRK cells in the presence or absence of extracellular calcium (D). Cellular pH was measured as previously described and pH recovery after sodium chloride re-addition was determined in the presence or absence of extracellular calcium (E). The bar graphs represent the average of 6 independent experiments for the indicated conditions and an average of 20 individual cell recordings were calculated per experiment. The traces indicate representative measurements (A, D). Data are displayed as mean ± S.E *P<0.05.

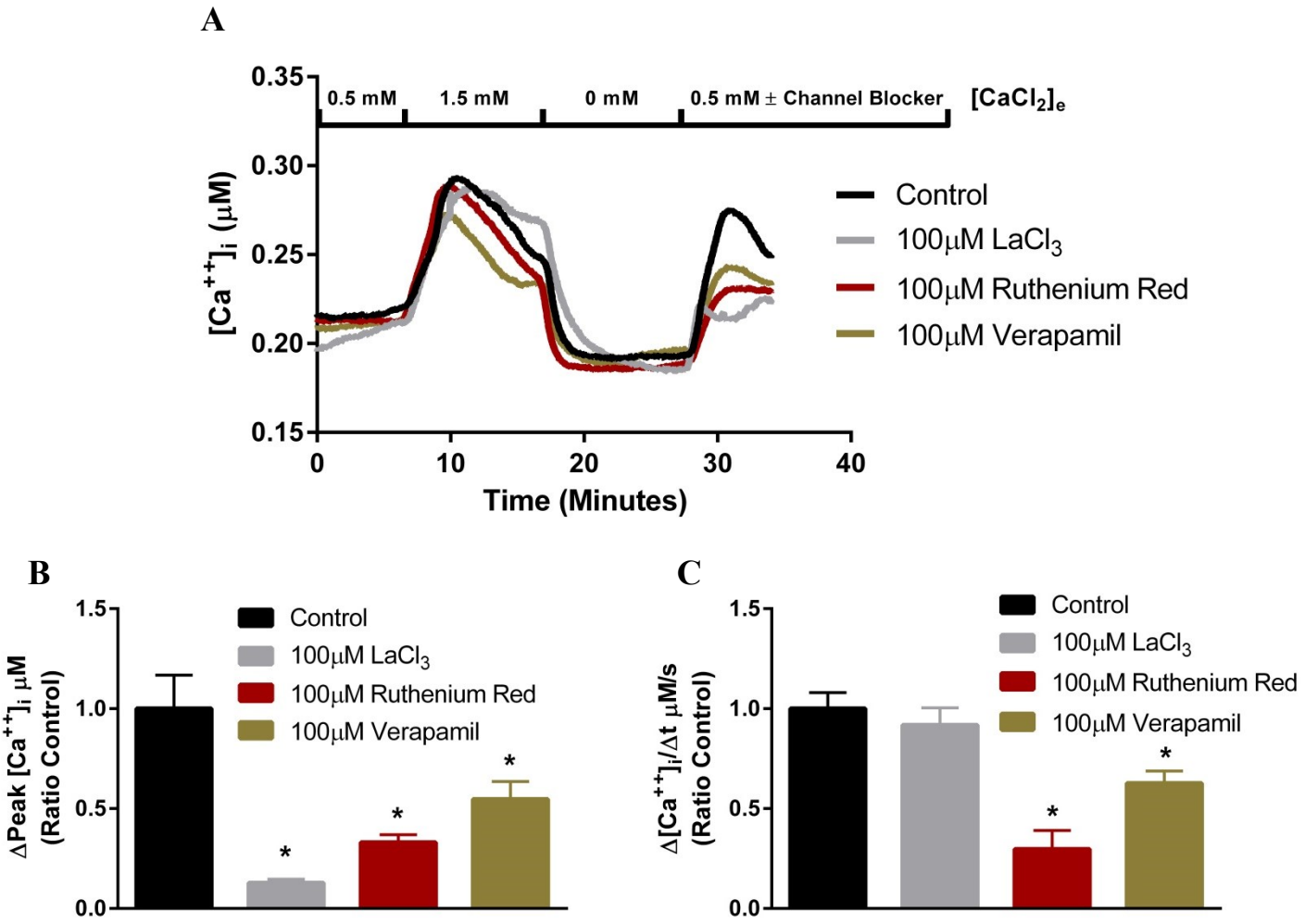

Figure 10) Calcium uptake in NRK cells is mediated by calcium channels: Calcium uptake was investigated in NRK cells using the method described in **Figure 8**. (A) Representative traces used to calculate two measurements: the change in peak from minimum extracellular calcium to maximum uptake after re-addition of 0.5 mM $CaCl_2$ (B) and the rate of calcium uptake during the first 15 sec after recovery (C). Calcium channel blockers were added during the uptake period as indicated. Lanthanum chloride is a divalent cation channel blocker, Ruthenium Red is a non-selective ion channel blocker, and Verapamil is a selective L-type calcium channel blocker. The bar graphs represent the average of 6 independent experiments for the indicated conditions and an average of 20 individual cell recordings were calculated per experiment. Data are displayed as mean ± S.E *P<0.05.

CHAPTER 4: DISCUSSION

4.1 NHE8 Expression Responds to Alterations in Calcium Homeostasis:

4.1.1 Mouse renal NHE8 mRNA and protein expression are discordant given the same treatment: The increase in protein levels despite reduced transcript of NHE8 appears contradictory. However, this is certainly not the first example of this phenomenon (Koussounadis *et al.,* 2015). Further investigation is required to understand these results. This may be a temporal effect where initially after treatment/activation of the CaSR there is a large increase in DNA transcription and subsequent increase in mRNA translation to synthesize new protein. Overtime, the protein remains but the mRNA might have been degraded and transcription of NHE8 gene attenuated. This is possible since mice were given vitamin D over a 5 day period and cinacalcet over 6 days (Dimke *et al.,* 2013). If NHE8 protein is stable at the plasma membrane during this time and sufficiently compensates for the perturbed calcium balance (possibly one of many other mechanisms), it would be an appropriate feedback response to degrade unnecessary NHE8 mRNA and stop new NHE8 mRNA transcription. This response may result in a reduction in total renal mRNA expression from baseline as was observed by qPCR **(Figure 2 A&B)**.

Using the cell culture model, we attempted to determine the half-life of NHE8 protein using cycloheximide, a bacterium derived toxin that has been used in research for decades as an inhibitor of protein biosynthesis (Ennis and Lubin 1964). We rationalized that determining the half-life of NHE8 would give insight to the possibility of the aforementioned hypothesis. However, the results of this experiment were inconclusive likely due to toxic effects on the cells. Furthermore, we hypothesized that perturbations to calcium homeostasis caused cellular stress, subsequent upregulation of heat shock proteins (HSPs), and stabilization of the NHE8 protein product. To test this, we examined alterations in the expression of HSPs by western blot. We found that HSP 25/27 protein levels were slightly but significantly increased whereas HSP 73

and HSP 90 protein levels were significantly reduced in the cinacalcet treated mice compared to controls (see appendix). Although the alterations in HSP expression raises new and interesting ideas, such as the possibility that cinacalcet attenuates basal physiologic stress within the kidneys, the results do not explain the difference between NHE8 mRNA and protein levels. This discussion will therefore focus on the alterations in NHE8 protein expression in response to perturbed calcium homeostasis in an animal model and potential lines of further inquiry for understanding the results.

4.1.2 NHE8 is regulated by activation of the CaSR: Renal NHE8 protein expression was increased in mice treated with cinacalcet, a calcimimetic acting to reduce plasma calcium concentration, and by vitamin D administration but NHE8 expression was not changed in response to altered calcium diets **(Figure 2)**. This response may be a direct consequence of activation of the CaSR in the kidney and subsequent cell signalling leading to altered gene and protein expression. Although controversial in the literature, CaSR mRNA was found in rat proximal tubules (Riccardi *et al.,* 1996) and protein localized to the apical brush border membrane of rat proximal tubule (Riccardi *et al.,* 1998/2000). It was later shown that the CaSR is also expressed in the proximal tubules of mice and human (Graca *et al.,* 2016). Thus it seems likely, given the predominance of NHE8 expression in the proximal tubule that we are observing alteration in NHE8 expression primarily in the proximal tubule. NHE8 gene expression regulated by activation of the CaSR via cinacalcet is consistent with the changes in NHE8 expression observed in the vitamin D treated mice. These mice had elevated levels of ionized plasma calcium which would have activated the proximal tubule CaSR. Further, mice on different calcium diets did not have alterations in plasma calcium levels and, consistent with the other treatment groups, no change in NHE8 mRNA expression. Taken together, the data suggest that

activation of the renal CaSR via increased plasma calcium concentration and cinacalcet leads to increased NHE8 protein expression in the renal proximal tubule.

4.1.3 NHE8 expression is unlikely regulated by changes in plasma calcium concentration independent of the CaSR: Given the results, it would be inconsistent to suggest NHE8 gene expression is being regulated by changes in plasma calcium by a CaSR independent mechanism. This is because NHE8 gene expression is decreased in both cinacalcet **(Figure 2A)** and vitamin D **(Figure 2B)** treated mice but these treatments result in a decrease and increase in plasma calcium concentration respectively (Dimke *et al.,* 2013). If the vitamin D treated group respond via a CaSR independent mechanism, it is most likely by the activation of the vitamin D receptor (VDR). However, animals treated with cinacalcet had no alteration in plasma vitamin D levels (Dimke *et al.,* 2013) so this does not explain those results. We must consider that the alterations in NHE8 expression in the vitamin D treated groups may be independent of changes in plasma calcium concentration and subsequent activation of the CaSR. In these mice, activation of the VDR may directly affect NHE8 expression thereby providing another level of receptor mediated regulation. The VDR receptor is expressed in the proximal tubule (Kumar *et al.,* 1994) but its role in regulating transport protein gene expression in this segment is unclear. It seems unlikely though that there would be two separate mechanisms increasing NHE8 expression given that in both experiments there would be CaSR activation.

4.1.4 NHE8 is possibly regulated by PTH: The results may be explained as a direct consequence of alterations in circulating PTH acting on the PTH receptor in the proximal tubule. In both cinacalcet and vitamin D treated mice, serum PTH levels are dramatically reduced compared to controls (Dimke *et al.,* 2013). The complex action of PTH in altering renal solute transport processes has been long appreciated (Dennis 1981). PTH primarily increases renal

calcium reabsorption via enhancing active transcellular uptake from the distal nephron (Agus *et al.,* 1993) and the cellular and molecular processes have more recently been elucidated (van Abel *et al.,* 2005). The role of PTH in proximal tubule calcium handling is poorly understood since the molecular transport mechanisms are largely undefined. It has been well established, however, that PTH downregulates NHE3 expression and transport activity in the proximal tubule through a variety of mechanisms (Bezerra *et al.,* 2008). Given the role of NHE3 in proximal tubule calcium reabsorption, these findings seem inconsistent and are discussed in greater detail elsewhere (Alexander *et al.,* 2013). If NHE8 is regulated similar to NHE3, then a reduction in serum PTH might allow an increase in NHE8 protein expression as observed in both cinacalcet **(Figure 2 D&E)** and vitamin D **(Figure 2 F&G)** treated mice. Given this reasoning, NHE8 would be predicted to attenuate calcium reabsorption or enhance calcium efflux from cells if PTH normally acts to suppress its expression and in its absence, NHE8 expression increases. This speculated role of NHE8 is consistent with our functional characterization of NHE8 in calcium handling discussed later.

4.2 Studying NHE8 Function in a Cell Culture Model:

4.2.1 NRK cells are a suitable model for studying NHE8: The suitability of the cell model for our purpose was determined based on a number of factors. First, we sought cells of mammalian origin and derived from renal proximal tubules. Importantly, these cells are not fibroblasts so they are able to polarize thereby discriminating an apical and basolateral membrane. NRK cells form tight junctions **(Figure 4A)** and leaky epithelia comparable to proximal tubules. These properties are important for studying transepithelial calcium flux. The

cells endogenously express NHE8 which we can study in a native environment lacking expression of NHE3, thus permitting us to discern NHE8 function alone (Zhang *et al.,* 2007). NHE3 is implicit to renal and intestinal calcium homeostasis (Pan *et al.,* 2012; Rievaj *et al.,* 2013) and the presence of NHE3 in experiments designed to investigate the role of NHE8 in calcium homeostasis would interfere with the results and potentially lead to false positives. Lastly, the cell line expresses NHE8 on the apical plasma membrane which allows functional analysis of this protein **(Figure 4 A&B;** Zhang *et al.,* 2007**)**. NRK cells met all these criteria. It is important to note that when we tried to overexpress NHE8 it accumulated in the golgi and did not traffic to the apical membrane of these cells precluding functional assessments. Taking the opposite approach, we were able to successfully KD NHE8 in NRK cells but the results were not reproducible and the viability of the cells was dramatically reduced (see appendix). We were, however, able to verify the 7A11 antibody specificity using this approach and found reduced NHE8 band intensity in the NHE8 siRNA treated group **(Figure 4C)**. We will try to create a knockout model to study NHE activity in this cell line by using CRISPR-Cas9 to delete NHE8 as a future direction.

4.2.2 Immunoblotting for NHE8: When immunoblotting with anti-NHE8 (7A11) antibody in both mouse kidney and NRK cells, three bands are detected. The higher molecular weight bands has been attributed to mature glycosylated NHE8 as it is abolished in cells treated with tunicamycin (Goyal *et al.,* 2003; see appendix). When NRK cells become confluent, protein levels of the low molecular weight NHE8 are reduced whereas the level of glycosylated NHE8 increases **(Figure 4D)**. These findings suggest that as NRK cells undergo a mesenchymal to epithelial transition, NHE8 is trafficked to the apical membrane moving from a predominantly endomembrane to plasma membrane localization. NHE8 apical expression in confluent NRK

cells was demonstrated using immunofluorescence confocal microscopy **(Figure 4A)**. Further, cell surface biotinylation experiments provide evidence for this reasoning since the lower molecular weight protein is undetected in confluent cells in either the total cell lysate or the surface biotin fraction **(Figure 4B)**. The functional role of endomembrane verses plasma membrane expressed NHE8 is unknown but since in mouse proximal tubules NHE8 localizes to the apical plasma membrane **(Figure 3)**, we decided to investigate calcium handling in NRK cells in the presence and absence of functional NHE8.

4.2.3 Functional characterization of NHE8 in NRK cells: Previous studies have shown, using reverse transcriptase PCR, that NRK cells exclusively express NHE8 and NHE1 (Zhang *et al.,* 2007). Since we were unable to over-express NHE8 or consistently KD NHE8 using siRNA, we decided to use the NHE inhibitor EIPA to inhibit NHE8. Using a sodium-dependant pH recovery assay, we could measure functional NHE activity in NRK cells if NHEs are expressed and function in the plasma membrane. We found that 1 μM EIPA is sufficient to attenuate all NHE activity in NRK cells **(Figure 5 A&B)**. We attributed these findings primarily to NHE8 for two main reasons: first, NHE1 is known to be expressed in the basolateral membranes of confluent NRK cells (Zhang *et al.,* 2007). Importantly, these studies were performed on confluent cells and as such basolaterally expressed NHE1 would not have been able to function. Second, in AP-1 cells over-expressing NHE1, they required a 10 fold greater amount of inhibitor, *i.e.* 10 μM EIPA to fully attenuate activity **(Figure 5 C&D)**. Together these results provide evidence that we can measure functional NHE activity primarily mediated by NHE8 in the apical membrane of confluent NRK cells providing an excellent model system to study the role of NHE8 in calcium handling.

4.3 The Cellular and Molecular Role for NHE8 in Calcium Handling:

4.3.1 Transepithelial calcium-45 flux is not affected by inhibition of NHE8 in NRK cells: Ion movement across an epithelium occurs either between the cells (paracellular), through the cells (transcellular) or a combination of both. Different nephron segments reabsorb calcium by different mechanisms. For instance, calcium is largely reabsorbed in a paracellular fashion in the PCT whereas in the DCT, calcium is reabsorbed transcellularly (Suki 1979). The method employed to measure transepithelial calcium flux does not discriminate between paracellular and transcellular calcium movement; however, since the TEER is relatively low in the proximal tubule, flux measured across confluent monolayers of this cell line are largely paracellular (Alexander *et al.,* 2014). Since inhibiting NHE8 with 100 μM EIPA does not alter transepithelial calcium flux **(Figure 6 A&B)**, the data suggests that NHE8 does not play a role in proximal tubule transepithelial calcium reabsorption via the paracellular route. Although there are further experiments required to invalidate a role for NHE8 in complete transepithelial movement of calcium, in particular the small fraction of transcellular calcium movement occurring across this segment (Suki 1979), these results did not give us any indication to further test our original hypothesis. The data does not, however, indicate that NHE8 has no role in handling calcium in any capacity.

4.3.2 NHE8 activity does not affect maximal calcium uptake in NRK cells: According to both our radionuclide studies and calcium imaging, maximal calcium uptake in NRK cells occurs within the first five mins after addition of extracellular calcium **(Figure 7A; Figure 8A)**. Using both techniques, we did not observe alterations in maximal calcium uptake in the presence or absence of functional NHE8. In addition, our kinetic analysis revealed the V_{max} between vehicle and EIPA treated cells is comparable **(Figure 7B)**. These results suggest that inhibition of NHE8

does not affect the maximal calcium uptake capacity in NRK cells. Similar results were observed for calcium uptake in the absence of extracellular sodium **(Figure 9A).** In sodium-free conditions, there is an increasing trend in maximal uptake however this increase is not significant **(Figure 9B)**. This discrepancy may be due to enhanced activity of the sodium/calcium exchanger (NCX) whereby removal of extracellular sodium causes intracellular sodium efflux and increased uptake of extracellular calcium in exchange. Given this rationale, NCX activity would have an additive effect to inhibition of NHE8 in mediating calcium uptake. To test this, we could simply repeat this experiment in the presence of the specific NCX inhibitor benzamil (Wang *et al.,* 2008) and see if the delta peak returns towards control. Importantly, inhibition of NHE8 would reduce intracellular sodium and thus attenuate calcium uptake into NRK cells by this mechanism. Thus, an effect on NCX is unlikely to explain the changes in calcium uptake rate observed.

4.3.3 NHE8 activity attenuates transient calcium uptake in NRK cells: Although there was not a statistically significant difference between the K_m or V_{max} of vehicle and EIPA treated cells, there was a nearly 30% decrease in the K_m for the EIPA treatment compared to vehicle **(Figure 7B)**. Since K_m is a measure of enzymatic or transport affinity, these results suggest that NRK cells may have a higher affinity for calcium uptake in the absence of NHE8 activity, i.e. the EIPA treated group requires less extracellular $CaCl_2$ to achieve the same rate of uptake. This reasoning is in agreement with our calcium imaging studies demonstrating enhanced calcium uptake in the absence of NHE8 activity by pharmacologic inhibition and by removal of the transporter substrate **(Figure 8&9)**. Together these findings suggest NHE8 plays a role in limiting transient calcium uptake.

From these results, we further speculated that if NHE8 attenuates calcium uptake basally, its transport activity is likely regulated by changes in extracellular calcium concentration. On the

contrary, we did not observe a difference in sodium-dependant pH recovery in NRK cells in the presence or absence of extracellular calcium **(Figure 9 D&E)**. These results suggest that NHE8 is not directly handling calcium and that it alters calcium uptake indirectly.

4.3.4 Extracellular pH affects calcium-45 uptake independently of NHE8 activity: In more alkaline extracellular pH, there is a significant increase in calcium uptake **(Figure 7C)**. There are a few lines of reasoning as to how this phenomenon may occur. First, NHE8 activity may alter calcium uptake, either enhancing influx or efflux, if NHE8 activity is regulated by extracellular or intracellular pH. This is consistent with the literature because NRK cells grown in acidic pH have increased NHE8 cell surface expression and activity (Joseph *et al.,* 2012). The authors, however, demonstrate that it requires a minimum 6 hrs of incubation in media of pH 6.6 to change NHE8 protein expression. These results do not provide insight into whether NHE8 activity is transiently regulated by extracellular pH. If NHE8 activity reduces calcium uptake, under acidic conditions, activated NHE8 could attenuate calcium uptake thereby providing an explanation for these findings. Interestingly, it is known that NHE1 activity is transiently increased in response to reduced cytosolic pH (Odunewu and Fliegel 2013) in renal cells. This response to sustained intracellular acidosis occurs via NHE1 phosphorylation and activation. Although the intracellular pH experienced by NHE8 was not determined for this experiment, this molecular regulatory mechanism may not be exclusive to NHE1. Evidence against this line of reasoning is that treatment with 1 μM EIPA does not affect this trend. If NHE8 activity is regulated by pH, which in turn affects calcium uptake, the treatment group would likely have steady calcium uptake at all buffered pHs. This leads to another line of reasoning which is that extracellular pH, possibly regulated by NHE8, alters calcium channel activity in the proximal tubule.

It has been shown that a variety of calcium channels are expressed in mammalian proximal tubules: L-type calcium channels have been observed in rabbit proximal tubules (Zhang *et al.,* 1996), the non-selective cation channel TRPC1 is expressed in rat proximal tubules (Goel *et al.,* 2005), and TRPV1 calcium channels are expressed in the PCT derived human kidney cell line, HK-2 cells (Jenkin *et al.,* 2010). These findings are consistent with our data demonstrating attenuated calcium uptake in NRK cells treated with calcium channel blockers **(Figure 10)**. Of these calcium channels, TRPV1 activity is well-known to be enhanced under acidic extracellular conditions (Bevan 2014). A role for pH regulated TRPV1 mediated calcium uptake in NRK cells is, however, inconsistent with our findings since calcium uptake is attenuated at acidic extracellular pH **(Figure 7C)**. Interestingly, evidence has been presented that transient intracellular alkalosis inhibits L-type calcium channel currents in a vascular smooth muscle cell line (Poteser *et al.,* 2003). Although these findings suggest calcium channel activity can be regulated by pH, without knowing intracellular pH conditions for our experiment we cannot draw any conclusions. To investigate this, we will repeat these experiments using the pH sensitive ratiometric fluorescent dye BCECF and see if intracellular pH changes and determine the relationship between calcium channel activity and intracellular pH alterations.

4.3.5 NHE8 unlikely mediates calcium efflux directly: Another possible interpretation of the data is that NHE8 is acting to transport sodium ions into the cells in exchange for calcium and protons. Thus, enhanced calcium uptake from the loss of NHE8 activity would occur if NHE8 is acting as a sodium/hydrogen/calcium exchanger **(Figure 11D)**. The purpose of this mechanism would most likely be to act as a shunt to prevent accumulation of intracellular calcium during calcium entry via the calcium channels. The NCX has a similar role in cardiomyocytes to remove intracellular calcium after cardiac contraction (Louch *et al.,* 2012). In

the proximal tubule, this may be physiologically important to keep cytosolic calcium at appropriate levels. Using EMBOSS Needle pairwise sequence alignment for proteins, mouse NHE8 has a 9.1% protein sequence identity with mouse NCX. The sequence identity is primarily between amino acids 120 – 576 of NHE8 and 20 – 408 of NCX. One method to test this hypothesis would be to measure NHE8 activity in the presence of the sarcoplasmic reticulum calcium ATPase inhibitor thapsigargin which increases cytosolic calcium transiently. If NHE8 has a role in calcium efflux as a means to prevent intracellular calcium accumulation, one would predict that NHE8 activity would increase under these conditions. However, we measured changes in cytosolic pH recovery after re-addition of extracellular sodium as NHE activity. This means we would also need to confirm that thapsigargin treatment does not itself alter cytosolic pH. Further, we can also alter cytosolic calcium using thapsigargin and see if the presence or absence of NHE8 function affects the cells ability to efflux the transient increase in cytosolic calcium.

4.3.6 NHE8 activity might regulate L-type calcium channel activity: As previously mentioned, inhibition of L-type calcium channels at alkaline cytosolic pH has been demonstrated. One possibility is that NHE8 may functionally interact with L-type channels by forming pH micro-domains. Given this, NHE8 activity in extruding intracellular protons in exchange for extracellular sodium may cause local and transient alkalization thereby attenuating calcium uptake via L-type channels. pH micro-domains are known to exist at the base of the brush border membrane in the proximal tubule and are established by the activity of NHE3 (Brasen *et al.,* 2014). Furthermore, is has also been shown that NHEs functionally interact with other membrane associated proteins such as the interaction between carbonic anhydrase II and NHE3 (Krishnan *et al.,* 2015). Given these findings, it is reasonable to speculate that NHE8 activity

may inhibit transient calcium influx by altering L-type calcium channel currents through functional interaction in plasma membrane micro-domains.

4.4 The role of NHE8 in Renal Calcium Reabsorption:

4.4.1 Summary and proposed model: Inhibition of NHE8 in NRK cells does not alter transepithelial calcium flux **(Figure 11A)**. However, the initial rate of calcium uptake is enhanced by inhibition of NHE8 in NRK cells. This mechanism is not mediated indirectly through NCX since removal of extracellular sodium enhances calcium uptake **(Figure 11B)**, (i.e. if present, NCX activity would lead to an attenuation of calcium uptake). Since calcium uptake is mediated by calcium channels in NRK cells, it is possible that the activity of NHE8 is either indirectly inhibiting calcium flux through these channels **(Figure 11C)** or directly providing an efflux mechanism to prevent accumulation of intracellular calcium **(Figure 11D)**.

NHE8 renal mRNA and protein expression is altered when calcium homeostasis is perturbed in mice. If these responses are due to activation of the CaSR, it is reasonable to assume that NHE8 protein is upregulated in a state of elevated plasma calcium since proximal tubular luminal calcium concentration is comparable to plasma and the CaSR is expressed at the brush border membrane of the proximal tubule (Riccardi *et al.,* 1996). In both the vitamin D and cinacalcet treated mice, urinary calcium excretion was elevated. This physiologic response is consistent with the speculation that NHE8 plays a role in apical membrane calcium efflux or attenuates calcium entry. Upregulation of NHE8 would therefore lead to reduced calcium uptake and thus increased luminal calcium and, depending on the response of the calcium handling machinery in the rest of the nephron, would ultimately lead to increased urine calcium excretion.

This may be a response under high extracellular conditions to protect the proximal tubule cells from cytotoxicity.

This speculation is largely based on the findings of a transcellular component of calcium reabsorption in the proximal tubule contributing significantly to overall calcium reabsorption in this nephron segment (Rouse *et al.,* 1980). The authors of this study microperfused rabbit isolated tubules and with the isotopic calcium-45 tracer, found that nearly 10% of filtered calcium is reabsorbed from the PST transcellularly. The transport machinery involved has not been elucidated. However, the aforementioned calcium channel could in theory mediate apical calcium influx. For transepithelial calcium reabsorption to occur, the cells would also need an intracellular calcium buffering or carrier protein mechanism to shuttle calcium to a basolateral calcium efflux mechanism similar to calcium handling by the DCT. $CaBP_{28k}$, for example, is expressed in the S1 segment of the proximal tubule (Lee *et al.,* 2015) and PMCA1 localizes in the caveolae of the proximal tubule basolateral membrane (Tortelote *et al.,* 2004) suggesting that the proximal tubule has the capacity for transcellular calcium reabsorption similar to the DCT.

4.4.2 Future directions: Measuring changes in intracellular calcium using fluorescence microscopy provides a powerful technique to investigate calcium handling in a cell model. We now need to determine which calcium channel(s) is mediating calcium entry into NRK cells and see if its activity is altered in the absence of NHE8. To this end, we need to repeat these functional studies when NHE8 is knocked out, potentially using CRISPR-Cas9 technology. To further elucidate a functional role for NHE8 in proximal tubule calcium reabsorption, calcium homeostasis in NHE8 knockout mice will be explored. These animals have been generated and demonstrate a mild phenotype with altered gastric epithelium and abnormal eye morphology. Calcium homeostasis has not been explored in these mice. We will measure intestinal calcium

uptake from these mice and urinary calcium excretion. In addition, we will investigate alterations in calcitropic hormone levels including PTH and vitamin D. The expression of potential compensatory pathways will also be explored by western blot and quantitative PCR. Ultimately these studies will delineate the role of NHE8 in calcium homeostasis and hopefully provide a novel target with which to manipulate calcium homeostasis thereby treating diseases of calcium mishandling.

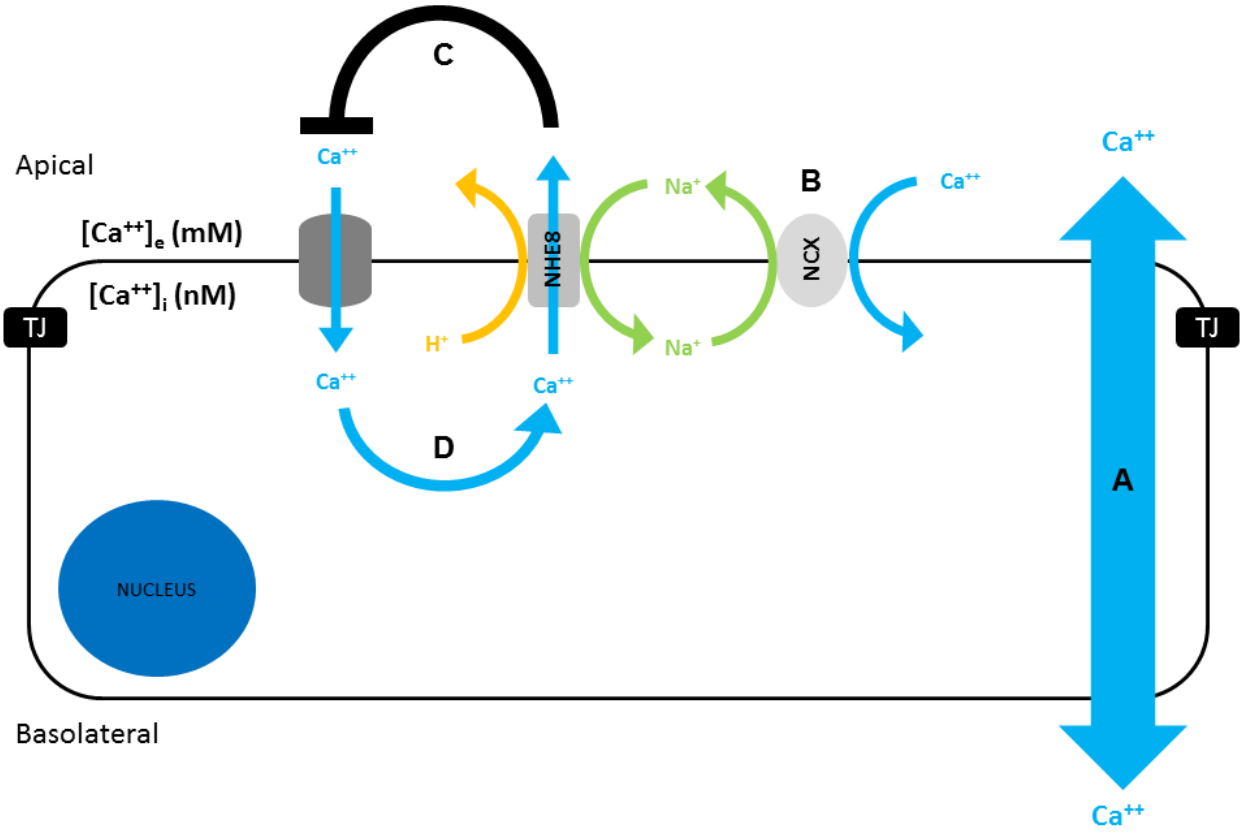

Figure 11) Proposed model of NHE8 mediated calcium efflux in NRK cells: A diagram illustrating apically expressed NHE8 in the renal proximal tubule cell and the potential roles NHE8 could play in calcium handling. (A) Transepithelial calcium movement involving both transcellular calcium transport and paracellular movement. (B) NHE8 activity working in collaboration with the sodium/calcium exchanger, NCX. (C) NHE8 activity inhibiting calcium uptake via a calcium channel. (D) NHE8 acts to efflux intracellular calcium directly.

BIBLIOGRAPHY

1. Abu Jawdeh BG, Khan S, Desche I, *et al*. Phosphoinositide binding differentially regulates NHE1 Na^+/H^+ exchanger-dependent proximal tubule cell survival. *J Biol Chem*. 2011; 286(49):42435-42445. doi:10.1074/jbc.M110.212845.

2. Agus ZS, Gardner LB, Beck LH, *et al*. Effects of parathyroid hormone on renal tubular reabsorption of calcium, sodium, and phosphate. *Am J Physiol*. 1973; 224(5):1143-1148.

3. Alexander RT, Dimke H, Cordat E. Proximal tubular NHEs: sodium, protons and calcium? *Am J Physiol Renal Physiol*. 2013; 305(3):F229-F236. doi:10.1152/ajprenal.00065.2013.

4. Alexander RT, Hemmelgarn BR, Wiebe N, *et al*. Kidney stones and kidney function loss: a cohort study. *Bmj*. 2012; 345(August):e5287. doi:10.1136/bmj.e5287.

5. Alexander RT, Hemmelgarn BR, Wiebe N, *et al*. Kidney stones and cardiovascular events: a cohort study. *Clin J Am Soc Nephrol*. 2014; 9(15):506-512. doi:10.2215/CJN.04960513.

6. Alexander RT, Rievaj J, Dimke H. Paracellular calcium transport across renal and intestinal epithelia. *Biochem Cell Biol*. 2014; 92(6):467-480. doi:10.1139/bcb-2014-0061.

7. Baum M. Developmental Changes in Rabbit Juxtamedullary Proximal Convoluted Tubule Acidification. *Pediatric Research.* 1992; 31(4):411-414.

8. Baum M, Twombley K, Gattineni J, *et al*. Proximal tubule Na^+/H^+ exchanger activity in adult $NHE8^{-/-}$, $NHE3^{-/-}$, and $NHE3^{-/-}/NHE8^{-/-}$ mice. *Am J Physiol Renal Physiol*. 2012; 303(11):F1495-F1502. doi:10.1152/ajprenal.00415.2012.

9. Beara-Lasic L, Edvardsson VO, Palsson R, *et al*. Genetic causes of kidney stones and kidney failure. *Clinic Rev Bone Miner Metab.* 2012; 10:2-18. doi:10.1007/s12018-011-9113-7.

10. Becker AM, Zhang J, Goyal S, *et al*. Ontogeny of NHE8 in the rat proximal tubule. *Am J Physiol - Ren Physiol*. 2007; 293(1):F255-F261. doi:10.1152/ajprenal.00400.2006.

11. Berndt TJ, Knox FG. Effects of parathyroid hormone and calcitonin on electrolyte excretion in the rabbit. *Kidney Int*. 1980; 17(4):473-478. doi:10.1038/ki.1980.55.

12. Bezerra CNA, Girardi ACC, Carraro-Lacroix LR, *et al*. Mechanisms underlying the long-term regulation of NHE3 by parathyroid hormone. *Am J Physiol Renal Physiol*. 2008; 294(5):F1232-F1237. doi:10.1152/ajprenal.00025.2007.

13. Biemesderfer D, Pizzonia J, Abu-Alfa a, *et al*. NHE3: a Na^+/H^+ exchanger isoform of renal brush border. *Am J Physiol*. 1993; 265:F736-F742.

14. Biemesderfer D, Reilly R, Exner M, *et al*. Immunocytochemical characterization of Na^+/H^+ exchanger isoform NHE1 in rabbit kidney. *Am J Physiol*. 1992; 263:833-840.

15. Biemesderfer D, Rutherford PA, Nagy T, *et al*. Monoclonal antibodies for high-resolution localization of NHE3 in adult and neonatal rat kidney. *Am J Physiol*. 1997; 273(2 Pt 2):F289-F299.

16. Bindels RJ. Calcium handling by the mammalian kidney. *J Exp Biol*. 1993; 184:89-104.

17. Bobulescu IA, Moe OW. Luminal Na^+/H^+ exchange in the proximal tubule. *Pflugers Arch Eur J Physiol*. 2009; 458(1):5-21. doi:10.1007/s00424-008-0595-1.

18. Bocanegra V, Gil Lorenzo AF, Cacciamani V, *et al*. RhoA and MAPKinase signal transduction pathways regulate NHE1 Na^+/H^+ exchanger-dependent proximal tubule cell apoptosis following mechanical stretch. *Am J Physiol Renal Physiol*. 2014:881-889. doi:10.1152/ajprenal.00232.2014.

19. Bomsztyk K, Wright FS. Dependence of ion fluxes on fluid transport by rat proximal tubule. *Am J Physiol*. 1986; 250:F680-F689.

20. Bookstein C, Xie Y, Rabenau K, *et al*. Tissue distribution of Na^+/H^+ exchanger isoforms NHE2 and NHE4 in rat intestine and kidney. *Am J Physiol*. 1997; 273(5 Pt 1):C1496-C1505.

21. Borghi L, Meschi T, Schianchi T, *et al*. Urine volume: stone risk factor and preventive measure. *Nephron*. 1999; 81:31-37. doi: 10.1159/000046296.

22. Borghi L, Schianchi T, Meschi T, *et* al. Comparison of two diets for the prevention of recurrent stones in idiopathic hypercalciuria. N *Engl J Med.* 2002; 346(2):1081-1090. doi:10.1056/NEJMoa012295.

23. Bourgeois S, Van Meer L, Wootla B, *et al*. NHE4 is critical for the renal handling of ammonia in rodents. *J Clin Invest*. 2010; 120(6):1895-1904. doi:10.1172/JCI36581.

24. Brasen JC, Burford JL, McDonough A, *et al*. Local pH domains regulate NHE3-mediated Na^+ reabsorption in the renal proximal tubule. *Am J Physiol Renal Physiol*. 2014; 307(11):F1249-F1262. doi:10.1152/ajprenal.00174.2014.

25. Brett CL, Donowitz M, Rao R. Evolutionary origins of eukaryotic sodium/proton exchangers. *Am J Physiol - Cell Physiol*. 2005; 288:C223-C239. doi:10.1152/ajpcell.00360.2004.

26. Brown EM, Gamba G, Riccardi D, *et al*. Cloning and characterization of an extracellular Ca^{2+}-sensing receptor from bovine parathyroid. *Nature*. 1993; 366(6455):575-580. doi:10.1038/366575a0.

27. Carney SL. Comparison of parathyroid hormone and calcitonin on rat renal calcium and magnesium transport. *Clincial Exp Pharmacol Physiol*. 1992; 19(I):433-438.

28. Chambrey R, St John PL, Eladari D, *et al*. Localization and functional characterization of Na^+/H^+ exchanger isoform NHE4 in rat thick ascending limbs. *Am J Physiol Renal Physiol*. 2001; 281(4):F707-F717.

29. Chambrey R, Warnock DG, Podevin R, *et al*. Immunolocalization of the Na^+/H^+ exchanger isoform NHE2 in rat kidney. *Am J Physiol*. 1998; 275(3 Pt 2):F379-F386.

30. Charoenphandhu N, Tudpor K, Pulsook N, *et al*. Chronic metabolic acidosis stimulated transcellular and solvent drag-induced calcium transport in the duodenum of female rats. *Am J Physiol Gastrointest Liver Physiol*. 2006; 291(3):G446-G455. doi:10.1152/ajpgi.00108.2006.

31. Chattopadhyay N, Cheng I, Rogers K, *et al*. Identification and localization of extracellular Ca^{2+} -sensing receptor in rat intestine. *Am. J. Physiol.* 1998; 274:122-130.

32. Choi JY, Shah M, Lee MG, *et al*. Novel amiloride-sensitive sodium-dependent proton secretion in the mouse proximal convoluted tubule. *J Clin Invest*. 2000; 105(8):1141-1146. doi:10.1172/JCI9260.

33. Civitelli R, Ziambaras K. Calcium and phosphate homeostasis: concerted interplay of new regulators. *J Endocrinol Invest*. 2011; 34(7 Suppl):3-7. doi:10.1080/07853890701689645.

34. Cochran M, Peacock M, Sachs G, *et al*. Renal effects of calcitonin. *Br Med J*. 1970; 1(5689):135-137.

35. Cole DE, Quamme G. Inherited disorders of renal magnesium handling. *J Am Soc Nephrol*. 2000; 11(3):1937-1947.

36. Collins JF, Honda T, Knobel S, *et al*. Molecular cloning, sequencing, tissue distribution, and functional expression of a Na^+/H^+ exchanger (NHE-2). *Proc. Natl. Acad. Sci. USA*. 1993; 90(May):3938-3942.

37. Curhan GC, Willett WC, Speizer FE, *et al*. Comparison of dietary calcium with supplemental calcium and other nutrients as factors affecting the risk of kidney stones in Women. *Ann Intern Med.* 1997; 126(7):497-504.

38. Curhan GC, Willett WC, Speizer FE, *et al*. Intake of vitamins B6 and C and the risk of kidney stones in women. *J Am Soc Nephrol*. 1999; 10(4):840-845. doi:10.1097/00005392-199905000-00125.

39. de Silva MG, Elliott K, Dahl H-H, *et al*. Disruption of a novel member of a sodium/hydrogen exchanger family and DOCK3 is associated with an attention deficit hyperactivity disorder-like phenotype. *J Med Genet*. 2003; 40(10):733-740. doi:10.1136/jmg.40.10.733.

40. Dennis VW. Actions of parathyroid hormone on isolated renal tubules. *Ann N Y Acad Sci*. 1981; 372:552-556.

41. Dent CE, Friedman M. Hypercalcuric Rickets Associated With Renal Tubular Damage. *Arch Dis Child*. 1964; 39:240-249. doi:10.1136/adc.39.205.240.

42. Di Stefano A, Roinel N, de Rouffignac C. Transepithelial Ca^{2+} and Mg^{2+} transport in the cortical thick ascending limb of Henle's loop of the mouse is a voltage-dependent process. *Ren Physiol Biochem*. 1993; 16:157-166.

43. Diering GH, Mills F, Bamji SX, *et al*. Regulation of dendritic spine growth through activity-dependent recruitment of the brain-enriched Na^+/H^+ exchanger NHE5. *Mol Biol Cell*. 2011; 22(13):2246-2257. doi:10.1091/mbc.E11-01-0066.

44. Dimke H, Desai P, Borovac J, *et al*. Activation of the Ca^{2+}-sensing receptor increases renal claudin-14 expression and urinary Ca^{2+} excretion. *Am J Physiol Renal Physiol*. 2013; 304(6):F761-F769. doi:10.1152/ajprenal.00263.2012.

45. Donowitz M, Ming Tse C, Fuster D. SLC9/NHE gene family, a plasma membrane and organellar family of Na^+/H^+ exchangers. *Mol Aspects Med*. 2013; 34(2-3):236-251. doi:10.1016/j.mam.2012.05.001.

46. Dudek SM, Chiang ET, Camp SM, *et al*. Abl tyrosine kinase phosphorylates non-muscle Myosin light chain kinase to regulate endothelial barrier function. *Mol Biol Cell*. 2010; 21(22):4042-4056. doi:10.1091/mbc.E09.

47. Eckermann-Ross C. Hormonal Regulation and Calcium Metabolism in the Rabbit. *Vet Clin North Am - Exot Anim Pract*. 2008; 11(1):139-152. doi:10.1016/j.cvex.2007.09.002.

48. Edvardsson, VO, Goldfarb DS, Lieske JC, *et al.* Hereditary causes of kidney stones and chronic kidney disease. *Pediatr Nephrol.* 2013; 28(10):1923-42. doi:10.1007/s00467-012-2329-z.

49. Eknoyan G, de Santo NG. The enlightenment kidney-nephrology in and about the eighteenth century. *Semin Dial*. 2012; 25(1):74-81. doi:10.1111/j.1525-139X.2011.00982.x.

50. Ennis HL, Lubin M. Cycloheximide: Aspects of Inhibition of Protein synthesis in Mammalian Cells. *Science*. 1964; 146(3650):1474-1476.

51. Evan A, Worcester E, Coe F, *et* al. Mechanisms of human kidney stone formation. *Urolithiasis.*2015; 43(0 1):19-32. doi:10.1007/s00240-014-0701-0.

52. Flocks RH. Calcium and phosphorus excretion in the urine of patients with renal ureteral calculi. *Jour. A.M.A.* 1939; 113(6):1466-1471

53. Favus M. Nephrolithiasis. [Updated 2013 Jul 1]. In: De Groot LJ, Beck-Peccoz P, Chrousos G, et al., editors. Endotext [Internet]. South Dartmouth (MA): MDText.com, Inc.; 2000-. Available from: http://www.ncbi.nlm.nih.gov/books/NBK279069/

54. Fisher SE, Black GC, Lloyd SE, *et al*. Isolation and partial characterization of a chloride channel gene which is expressed in kidney and is a candidate for Dent's disease (an X-linked hereditary nephrolithiasis). *Hum Mol Genet*. 1994; 3(11):2053-2059.

55. Franceschini N, Joy MS, Kshirsagar A. Cinacalcet HCl: a calcimimetic agent for the management of primary and secondary hyperparathyroidism. *Expert Opin Investig Drugs*. 2003; 12(8):1413-1421. doi:10.1517/13543784.12.8.1413.

56. Friedman P, Gesek F. Cellular calcium transport in renal epithelia: measurement, mechanisms, and regulation. *The American Physiological Society*. 1995; 75(3):429-471.

57. Fuster DG, Alexander RT. Traditional and emerging roles for the SLC9 Na^+/H^+ exchangers. *Pflugers Arch Eur J Physiol*. 2014; 466(1):61-76. doi:10.1007/s00424-013-1408-8.

58. Gilfillan GD, Selmer KK, Roxrud I, *et al*. SLC9A6 Mutations Cause X-Linked Mental Retardation, Microcephaly, Epilepsy, and Ataxia, a Phenotype Mimicking Angelman Syndrome. *Am J Hum Genet*. 2008; 82(4):1003-1010. doi:10.1016/j.ajhg.2008.01.013.

59. Goel M, Sinkins WG, Zuo C, *et al*. Identification and localization of TRPC channels in the rat kidney. *Am J Physiol Ren Physiol*. 2006; 1998:1241-1252. doi:10.1152/ajprenal.00376.2005.

60. Good DW, George T, Watts BA. High sodium intake increases HCO^{3-} absorption in medullary thick ascending limb through adaptations in basolateral and apical Na^+/H^+ exchangers. *Am J Physiol Physiol*. 2011; 301(2):F334-F343. doi:10.1152/ajprenal.00106.2011.

61. Good DW, Watts 3rd BA, George T, *et al*. Transepithelial HCO^{3-} absorption is defective in renal thick ascending limbs from Na^+/H^+ exchanger NHE1 null mutant mice. *Am J Physiol Ren Physiol*. 2004; 287(6):F1244-F1249. doi:10.1152/ajprenal.00176.2004.

62. Goyal S, Mentone S, Aronson PS. Immunolocalization of NHE8 in rat kidney. *Am J Physiol Renal Physiol*. 2005; 288(3):F530-F538. doi:10.1152/ajprenal.00229.2004.

63. Goyal S, Vanden Heuvel G, Aronson PS. Renal expression of novel Na^+/H^+ exchanger isoform NHE8. *Am J Physiol Renal Physiol*. 2003; 284(3):F467-F473. doi:10.1152/ajprenal.00352.2002.

64. Graca JAZ, Schepelmann M, Brennan SC, *et al*. Comparative expression of the extracellular calcium-sensing receptor in the mouse, rat, and human kidney. *Am J Physiol - Ren Physiol*. 2016; 310(6):F518-F533. doi:10.1152/ajprenal.00208.2015.

65. Grynkiewicz G, Poenie M, Tsien RY. A new generation of Ca^{2+} indicators with greatly improved fluorescence properties. *J Biol Chem*. 1985; 260(6):3440-3450. doi:3838314.

66. Hanner F, Chambrey R, Bourgeois S, *et al*. Increased renal renin content in mice lacking the Na^+/H^+ exchanger NHE2. *Am J Physiol Ren Physiol*. 2008; 294(4):F937-F944. doi:00591.2007 [pii]\n10.1152/ajprenal.00591.2007.

67. Hoenderop JG, Müller D, Suzuki M, *et al*. Epithelial calcium channel: gate-keeper of active calcium reabsorption. *Curr Opin Nephrol Hypertens*. 2000; 9(4):335-340. doi:10.1097/00041552-200007000-00003.

68. Hoenderop JG, Müller D, Van Der Kemp a W, *et al*. Calcitriol controls the epithelial calcium channel in kidney. *J Am Soc Nephrol*. 2001; 12:1342-1349.

69. Hoenderop J. Renal Ca^{2+} wasting, hyperabsorption, and reduced bone thickness in mice lacking TRPV5. *J Clin Invest*. 2003; 112(12):1906-1914. doi:10.1172/JCI19826.The.

70. Hoenderop J, Dardenne O, Van Abel M, *et al*. Modulation of renal Ca^{2+} transport protein genes by dietary Ca^{2+} and 1,25-dihydroxyvitamin D3 in 25-hydroxyvitamin D3-1alpha-hydroxylase knockout mice. *FASEB J*. 2002; 16:1398-1406. doi:10.1096/fj.02-0225com.

71. Hoenderop J, Nilius B, Bindels RJM. Calcium absorption across epithelia. *Physiol Rev*. 2005; 85(1):373-422. doi:10.1152/physrev.00003.2004.

72. Hoenderop J, van der Kemp AWCM, Hartog A, *et al*. Molecular identification of the apical Ca^{2+} channel in 1,25-Dihydroxyvitamin D_3-responsive epithelia. *JBC.* 1999; 274(13):8375-8378.

73. Holmes RP, Assimos DG. The impact of dietary oxalate on kidney stone formation. *Urol Res*. 2004; 32(5):311-316. doi:10.1007/s00240-004-0437-3.

74. Hou J, Renigunta A, Konrad M, *et al*. Claudin-16 and claudin-19 interact and form a cation-selective tight junction complex. *J Clin Invest*. 2008; 118(2):619-628. doi:10.1172/JCI33970.

75. Jenkin KA, McAinch AJ, Grinfeld E, *et al*. Role for cannabinoid receptors in human proximal tubular hypertrophy. *Cell Physiol Biochem*. 2010; 26:879-886. doi:10.1159/000323997.

76. Joseph C, Twombley K, Gattineni J, *et al*. Acid increases NHE8 surface expression and activity in NRK cells. *Am J Physiol Ren Physiol*. 2012; 302(4):F495-F503. doi:10.1152/ajprenal.00331.2011.

77. Khan S, Jawdeh BGA, Goel M, *et al*. Lipotoxic disruption of NHE1 interaction with PI(4,5)P2 expedites proximal tubule apoptosis. *J Clin Invest*. 2014; 124(3):1057-1068. doi:10.1172/JCI71863.

78. Khosla S, Ebeling PR, Firek AF, *et al*. Calcium infusion suggests a "set-point" abnormality of parathyroid gland function in familial benign hypercalcemia and more complex disturbances in primary hyperparathyroidism. *J Clin Endocrinol Metab*. 1993; 76(3):715-720. doi:10.1210/jcem.76.3.8445032.

79. Klanke CA, Su YR, Callen DF, *et al*. Molecular cloning and physical and genetic mapping of a novel human Na^+/H^+ exchanger (NHE5/SLC9A5) to chromosome 16q22.1. *Genomics*. 1995; 25(3):615-622. doi:10.1016/0888-7543(95)80002-4.

80. Kochanek KD, Xu J, Murphy SL, *et al*. National Vital Statistics Reports Deaths : Final Data for 2009. *Natl Cent Heal Stat*. 2012; 60(3):1-117.

81. Kondapalli KC, Hack A, Schushan M, *et al*. Functional evaluation of autism-associated mutations in NHE9. *Nat Commun*. 2013; 4(May):2510. doi:10.1038/ncomms3510.

82. Konrad M, Schaller A, Seelow D, *et al*. Mutations in the tight-junction gene claudin 19 (CLDN19) are associated with renal magnesium wasting, renal failure, and severe ocular involvement. *Am J Hum Genet*. 2006; 79(5):949-957. doi:10.1086/508617.

83. Koussounadis A, Langdon SP, Um IH, *et al*. Relationship between differentially expressed mRNA and mRNA-protein correlations in a xenograft model system. *Sci Rep*. 2015; 5(May):10775. doi:10.1038/srep10775.

84. Krishnan D, Liu L, Wiebe SA, *et al*. Carbonic anhydrase II binds to and increases the activity of the epithelial sodium proton exchanger, NHE3. *Am J Physiol Renal Physiol*. 2015; 309(4):ajprenal.00464.2014. doi:10.1152/ajprenal.00464.2014.

85. Kumar R, Schaefer J, Grande JP, *et al*. Immunolocalization of calcitriol receptor, 24-hydroxylase cytochrome P-450, and calbindin D28k in human kidney. *Am J Physiol*. 1994; 266:F477-F485.

86. LaBonne C, Bronner-Fraser M. Molecular mechanisms of neural crest formation. *Annu Rev Cell Dev Biol*. 1999; 15(1):81-112. doi:10.1146/annurev.cellbio.15.1.81.

87. Lapointe JY, Laprade R, Cardinal J. Transepithelial and cell membrane electrical resistances of the rabbit proximal convoluted tubule. *Am J Physiol*. 1984; 247(4 Pt 2):F637-F649.

88. Lassiter WE, Gottschalk CW, Mylle M. Micropuncture study of renal tubular reabsorption of calcium in normal rodents. *Am. J. Physiol.* 1963; 204(5):771-775.

89. Lawson DEM, Fraser DR, Kodicek E, *et al*. Identification of 1,25-Dihydroxycholecalciferol: a New Kidney Hormone controlling Calcium Metabolism. *Nature*. 1971; 230(March):228-230. doi:10.1038/230228a0.

90. Lee AJ, Chen YH, Chu ML, *et al*. Effect of hydrochlorothiazide on renal calcium and sodium excretion of different ages (III). *Zhonghua Min Guo Xiao Er Ke Yi Xue Hui Za Zhi*. 1994; 35(4):306-311.

91. Lee JW, Chou C-L, Knepper M. Deep Sequencing in Microdissected Renal Tubules Identifies Nephron Segment-Specific Transcriptomes. *J Am Soc Nephrol*. 2015:1-9. doi:10.1681/ASN.2014111067.

92. Lemann J, Worcester EM, Gray RW. Hypercalciuria and Stones. *Am J Kidney Dis*. 1991; 17(4):386-391. doi:10.1016/S0272-6386(12)80628-7.

93. Li HC, Du Z, Barone S, *et al*. Proximal tubule specific knockout of the Na^+/H^+ exchanger NHE3: Effects on bicarbonate absorption and ammonium excretion. *J Mol Med*. 2013; 91(8):951-963. doi:10.1007/s00109-013-1015-3.

94. Litwin M, Saigal C. Urinary Tract Stones. In: *Urologic Diseases in America*. Washington, D.C.: NIH publication; 2012.

95. Louch WE, Stokke MK, Sjaastad I, *et al*. No Rest for the Weary: Diastolic Calcium Homeostasis in the Normal and Failing Myocardium. *Physiology*. 2012; 27(5):308-323. doi:10.1152/physiol.00021.2012.

96. Malakooti J, Dahdal RY, Schmidt L, *et al*. Molecular cloning, tissue distribution, and functional expression of the human Na^+/H^+ exchanger NHE2. *Am J Physiol*. 1999; 277:G383-G390.

97. Mattei M, Sardet C, Franchi A, *et al*. The human amiloride-sensitive Na^+/H^+ antiporter: localization to chromosome 1 by in situ hybridization. *Cytogenet Cell Genet*. 1988; 48(1):6-8.

98. McGeown M. Heredity in renal stone disease. *Clin Sci*. 1960; 19:465-471.

99. Mercer PF, Maddox DA, Brenner BM. Current concepts of sodium chloride and water transport by the mammalian nephron. *West J Med*. 1974; 120(1):33-45.

100. Miederer A-M, Alansary D, Schwär G, *et al*. A STIM2 splice variant negatively regulates store-operated calcium entry. *Nat Commun*. 2015; 6:6899. doi:10.1038/ncomms7899.

101. Monga M. Climate-related increase in the prevalence of urolithiasis in the United States: Editorial comment. *Int Braz J Urol*. 2008; 34(4):517. doi:10.1073/pnas.0709652105.

102. Morrow EM, Yoo SY, Flavell SW, *et al*. Identifying autism loci and genes by tracing recent shared ancestry. *Science*. 2008; 321:218-223.

103. Müller D, Hoenderop JGJ, Meij IC, *et al*. Molecular Cloning, Tissue Distribution, and Chromosomal Mapping of the Human Epithelial Ca^{2+} Channel (ECAC1). *Genomics*. 2000; 67(1):48-53. doi:10.1006/geno.2000.6203.

104. Müller D, Hoenderop JGJ, Vennekens R, *et al*. Epithelial Ca^{2+} channel (ECAC1) in autosomal dominant idiopathic hypercalciuria. *Nephrol Dial Transplant*. 2002; 17(9):1614-1620.

105. Mullins LJ, Bailey MA, Mullins JJ. Hypertension, Kidney, and Transgenics: A Fresh Perspective. *Physiol Rev.* 2006; 86:709-746. doi:10.1152/physrev.00016.2005.

106. Mundy GR, Guise T. Hormonal control of calcium homeostasis. *Clin Chem*. 1999; 45(8 Pt 2):1347-1352.

107. Murayama Y, Morel F, Le Grimellec C. Phosphate, calcium and magnesium transfers in proximal tubules and loops of henle, as measured by single nephron microperfusion experiments in the rat. *Pflügers Arch Eur J Physiol*. 1972; 333(1):1-16. doi:10.1007/BF00586037.

108. Murer H, Hopfer U, Kinne R. Sodium/proton antiport in brush-border-membrane vesicles isolated from rat small intestine and kidney. *Biochem J*. 1976; 154(3):597-604.

109. Nakamura N, Tanaka S, Teko Y, *et al*. Four Na^+/H^+ exchanger isoforms are distributed to Golgi and post-Golgi compartments and are involved in organelle pH regulation. *J Biol Chem*. 2005; 280(2):1561-1572. doi:10.1074/jbc.M410041200.

110. Ng RCK, Rouse D, Suki WN. Calcium transport in the rabbit superficial proximal convoluted tubule. *J Clin Invest*. 1984; 74(3):834-842. doi:10.1172/JCI111500.

111. Nilius B, Flockerzi V. Mammalian Transient Receptor Potential (TRP) Cation Channels. *Volume II*. Vol 223; 2014. doi:10.1007/978-3-319-05161-1.

112. Nouvenne A, Meschi T, Prati B, *et al*. Effects of a low-salt diet on idiopathic hypercalciuria in calcium-oxalate stone formers: A 3-mo randomized controlled trial. *Am J Clin Nutr*. 2010; 91(3):565-570. doi:10.3945/ajcn.2009.28614.

113. Numata M, Orlowski J. Molecular cloning and characterization of a novel (Na^+, K^+)/H^+ exchanger localized to the trans-Golgi network. *J Biol Chem*. 2001; 276(20):17387-17394. doi:10.1074/jbc.M101319200.

114. Numata M, Petrecca K, Lake N, *et al*. Identification of a Mitochondrial Na^+ / H^+ Exchanger. *JBC.* 1998; 273(12):6951-6959.

115. Odunewu A, Fliegel L. Acidosis-mediated regulation of the NHE1 isoform of the Na^+/H^+ exchanger in renal cells. *Am J Physiol Renal Physiol*. 2013; 305(3):F370-F381. doi:10.1152/ajprenal.00598.2012.

116. Okano T, Tsugawa N, Morishita A, *et al*. Regulation of gene expression of epithelial calcium channels in intestine and kidney of mice by 1alpha,25-dihydroxyvitamin D3. *J Steroid Biochem Mol Biol*. 2004; 89-90(1-5):335-338. doi:10.1016/j.jsbmb.2004.03.024.

117. Onishi I, Lin PJC, Numata Y, *et al*. Organellar (Na^+, K^+)/H^+ exchanger NHE7 regulates cell adhesion, invasion and anchorage-independent growth of breast cancer MDA-MB-231 cells. *Oncol Rep*. 2012; 27(2):311-317. doi:10.3892/or.2011.1542.

118. Orlowski J, Kandasamy RA, Shull GE. Molecular cloning of putative members of the Na/H exchanger gene family. cDNA cloning, deduced amino acid sequence, and mRNA tissue expression of the rat Na^+/H^+ exchanger NHE1 and two structurally related proteins. *J Biol Chem*. 1992; 267(13):9331-9339.

119. Orlowski J, Grinstein S. Diversity of the mammalian sodium/proton exchanger SLC9 gene family. *Pflugers Arch Eur J Physiol*. 2004; 447(5):549-565. doi:10.1007/s00424-003-1110-3.

120. Pak CY, Sakhaee K, Fuller CJ. Physiological and physiochemical correction and prevention of calcium stone formation by potassium citrate therapy. *Trans Assoc Am Physicians*. 1983; 96:294-305.

121. Pan W, Borovac J, Spicer Z, *et al*. The epithelial sodium/proton exchanger, NHE3, is necessary for renal and intestinal calcium (re)absorption. *Am J Physiol Renal Physiol*. 2012; 302(8):F943-F956. doi:10.1152/ajprenal.00504.2010.

122. Peacock M, Nordin BE. Tubular reabsorption of calcium in normal and hypercalciuric subjects. *J Clin Pathol*. 1968; 21(3):353-358.

123. Pearle M, Calhoun E, CurhanG. Urologic Diseases in America Project: Urolithiasis. *J Urol*. 2005; 173(3):848-857. doi:10.1097/01.ju.0000152082.14384.d7.

124. Pearle MS, Goldfarb DS, Assimos DG, *et al*. Medical management of kidney stones: AUA guideline. *J Urol*. 2014; 192(2):316-324. doi:10.1016/j.juro.2014.05.006.

125. Peti-Peterdi J, Chambrey R, Bebok Z, *et al*. Macula densa Na^+/H^+ exchange activities mediated by apical NHE2 and basolateral NHE4 isoforms. *Am J Physiol Renal Physiol*. 2000; 278(3):F452-F463.

126. Pirojsakul K, Gattineni J, Dwarakanath V, *et al*. Renal NHE expression and activity in neonatal NHE3- and NHE8-null mice. *AJP Ren Physiol*. 2015; 308(1):F31-F38. doi:10.1152/ajprenal.00492.2014.

127. Pitts RF, Lotspeich WD, Schiess WA, *et al*. the Renal Regulation of Acid-Base Balance in Man. I. the Nature of the Mechanism for Acidifying the Urine. *J Clin Invest*. 1948; 27(1):48-56. doi:10.1172/JCI101923.

128. Pitts TO, McGowan JA, Chen TC, *et al*. Inhibitory effects of volume expansion performed in vivo on transport in the isolated rabbit proximal tubule perfused in vitro. *J Clin Invest*. 1988; 81(4):997-1003. doi:10.1172/JCI113454.

129. Pizzonia JH, Biemesderfer D, Abu-Alfa AK, *et al*. Immunochemical characterization of Na^+/H^+ exchanger isoform NHE4. *Am J Physiol*. 1998; 275(4 Pt 2):F510-F517.

130. Poteser M, Wakabayashi I, Rosker C, *et al*. Crosstalk between voltage-independent Ca^{2+} channels and L-type Ca^{2+} channels in A7r5 vascular smooth muscle cells at elevated intracellular pH: Evidence for functional coupling between L-type Ca^{2+} channels and a 2-

APB-sensitive cation channel. *Circ Res*. 2003; 92(8):888-896. doi:10.1161/01.RES.0000069216.80612.66.

131. Pouysségur J, Chambard JC, Franchi A, *et al*. Growth factor activation of an amiloride-sensitive Na^+/H^+ exchange system in quiescent fibroblasts: coupling to ribosomal protein S6 phosphorylation. *Proc Natl Acad Sci USA*. 1982; 79(13):3935-3939. doi:10.1073/pnas.79.13.3935.

132. Preisig PA, Ives HE, Cragoe EJ, *et al*. Role of the Na^+/H^+ antiporter in rat proximal tubule bicarbonate absorption. *J Clin Invest*. 1987; 80(4):970-978. doi:10.1172/JCI113190.

133. Quamme GA. Effect of calcitonin on calcium and magnesium absorption in rat nephron. *Am J Physiol*. 1980; 238:E573-E578.

134. Rector FC. Sodium, bicarbonate, and chloride absorption by the proximal tubule. *Am J Physiol.* 1983; 244(13):F461-F471.

135. Renkema KY, Lee K, Topala CN, *et al*. TRPV5 gene polymorphisms in renal hypercalciuria. *Nephrol Dial Transplant*. 2009; 24(6):1919-1924. doi:10.1093/ndt/gfn735.

136. Resnick M, Pridgen DB, Goodman HO. Genetic Predisposition to Formation of Calcium Oxalate Renal Calculi. *N Engl J Med*. 1968; 278:1313-1318.

137. Reuss L, Finn AL. Passive Electrical Properties of Toad Urinary Bladder Epithelium Intercellular Electrical Coupling and Transepithelial Cellular and Shunt Conductances. *Journal of General Physiology.* 1974; 64:1-25.

138. Riccardi D, Hall AE, Chattopadhyay N, *et al*. Localization of the extracellular Ca^{2+}/polyvalent cation-sensing protein in rat kidney. *Am J Physiol*. 1998; 274(3 Pt 2):F611-F622.

139. Riccardi D, Park J, Lee WS, *et al*. Cloning and functional expression of a rat kidney extracellular calcium/polyvalent cation-sensing receptor. *Proc Natl Acad Sci USA*. 1995; 92(1):131-135. doi:10.1073/pnas.92.1.131.

140. Riccardi D, Traebert M, Ward D, *et al*. Dietary phosphate and parathyroid hormone alter the expression of the calcium-sensing receptor (CaR) and the Na^+-dependent P_i

transporter (NaPi-2) in the rat proximal tubule. *Pflugers Arch Eur J Physiol*. 2000; 441(2-3):379-387.

141. Riccardi D, Lee WS, Lee K, *et al*. Localization of the extracellular Ca^{2+}-sensing receptor and PTH/PTHrP receptor in rat kidney. *Am J Physiol*. 1996; 271(4 Pt 2):F951-F956.

142. Rievaj J, Pan W, Cordat E, *et al*. The Na^+/H^+ exchanger isoform 3 is required for active paracellular and transcellular Ca^{2+} transport across murine cecum. *Am J Physiol Gastrointest Liver Physiol*. 2013; 305(4):G303-G313. doi:10.1152/ajpgi.00490.2012.

143. Rouse D, Ng RCK, Suki WN. Calcium transport in the pars recta and thin descending limb of Henle of the rabbit, perfused in vitro. *J Clin Invest*. 1980; 65(1):37-42. doi:10.1172/JCI109657.

144. Ruat M, Molliver ME, Snowman a M, *et al*. Calcium sensing receptor: molecular cloning in rat and localization to nerve terminals. *Proc Natl Acad Sci USA*. 1995; 92(8):3161-3165. doi:10.1073/pnas.92.8.3161.

145. Rutherford P, Pizzonia JH, Biemesderfer D, *et al*. Expression of Na^+/H^+ exchanger isoforms NHE1 and NHE3 in kidney and blood cells of rabbit and rat. *Exp Nephrol*. 1997; 5(6):490-497.

146. Sardet C, Franchi A, Pouyssegur J. Molecular Cloning, Primary Structure, and Expression of the Human Growth Factor-Activatable Na^+/H^+ Antiporter. *Cell.* 1989; 56:271-280.

147. Scales CD, Smith AC, Hanley JM, *et al*. Prevalence of kidney stones in the United States. *Eur Urol*. 2012; 62(1):160-165. doi:10.1016/j.eururo.2012.03.052.

148. Schnittler HJ. Structural and functional aspects of intercellular junctions in vascular endothelium. *Basic Res Cardiol*. 1998; 93 Suppl 3:30-39.

149. Schultheis PJ, Clarke LL, Meneton P, *et al*. Renal and intestinal absorptive defects in mice lacking the NHE3 Na^+/H^+ exchanger. *Nat Genet*. 1998; 19(3):282-285. doi:10.1038/969.

150. Schultheis PJ, Clarke LL, Meneton P, *et al*. Targeted disruption of the murine Na^+/H^+ exchanger isoform 2 gene causes reduced viability of gastric parietal cells and loss of net acid secretion. *J Clin Invest*. 1998; 101(6):1243-1253. doi:10.1172/JCI1249.

151. Seely JF, Dirks JH. Micropuncture study of hypertonic mannitol diuresis in the proximal and distal tubule of the dog kidney. *J Clin Invest*. 1969; 48(12):2330-2340. doi:10.1172/JCI106199.

152. Simon DB. Paracellin-1, a renal tight junction protein required for paracellular Mg^{2+} resorption. *Science*. 1999; 285(5424):103-106. doi:10.1126/science.285.5424.103.

153. Stechman MJ, Loh NY, Thakker R V. Genetic causes of hypercalciuric nephrolithiasis. *Pediatr Nephrol*. 2009; 24(12):2321-2332. doi:10.1007/s00467-008-0807-0.

154. Suki WN. Calcium transport in the nephron. *Am J Physiol*. 1979; 237(l):F1-F6. doi:10.1146/annurev.ph.41.030179.001325.

155. Sweny P. Medical management of renal transplantation. *Medicine (Baltimore)*. 2007; 35(9):483-488. doi:10.1016/j.mpmed.2007.06.011.

156. Tang J, Chonchol MB. Vitamin D and kidney stone disease. *Curr Opin Nephrol Hypertens*. 2013; 22(4):383-389. doi:10.1097/MNH.0b013e328360bbcd.

157. Tanrattana C, Charoenphandhu N, Limlomwongse L, *et al*. Prolactin directly stimulated the solvent drag-induced calcium transport in the duodenum of female rats. *Biochim Biophys Acta - Biomembr*. 2004; 1665(1-2):81-91. doi:10.1016/j.bbamem.2004.06.017.

158. Topala CN, Schoeber JPH, Searchfield LE, *et al*. Activation of the Ca^{2+}-sensing receptor stimulates the activity of the epithelial Ca^{2+} channel TRPV5. *Cell Calcium*. 2009; 45(4):331-339. doi:10.1016/j.ceca.2008.12.003.

159. Torres PU. Cinacalcet HCl: a novel treatment for secondary hyperparathyroidism caused by chronic kidney disease. *J Ren Nutr*. 2006; 16(3):253-258. doi:10.1053/j.jrn.2006.04.010.

160. Tortelote GG, Valverde RHF, Lemos T, *et al*. The plasma membrane Ca^{2+} pump from proximal kidney tubules is exclusively localized and active in caveolae. *FEBS Lett*. 2004; 576(1-2):31-35. doi:10.1016/j.febslet.2004.08.055.

161. Traxer O, Huet B, Poindexter J, *et al*. Effect of Ascorbic Acid Consumption On Urinary Stone Risk Factors. *J Urol*. 2003; 170(2):397-401. doi:10.1097/01.ju.0000076001.21606.53.

162. Tse CM, Levine S, Yun CH, *et al*. Functional characteristics of a cloned epithelial Na^+/H^+ exchanger (NHE3): resistance to amiloride and inhibition by protein kinase C. *Proc Natl Acad Sci USA*. 1993; 90(19):9110-9114.

163. Tse CM, Brant SR, Walker MS, *et al*. Cloning and sequencing of a rabbit cDNA encoding an intestinal and kidney-specific Na^+/H^+ exchanger isoform (NHE3). *J Biol Chem*. 1992; 267(13):9340-9346.

164. Tudpor K, Teerapornpuntakit J, Jantarajit W, *et al*. 1,25-dihydroxyvitamin D(3) rapidly stimulates the solvent drag-induced paracellular calcium transport in the duodenum of female rats. *J Physiol Sci*. 2008; 58(5):297-307. doi:10.2170/physiolsci.RP002308.

165. Ullrich KJ, Rumrich G, Kloss S. Active Ca^{2+} Reabsorption in the Proximal Tubule of the Rat Kidney. *Pflugers Arch.* 1976; 364:223-228.

166. Ullrich KJ, Schmidt-Nielson B, O'Dell R, *et al*. Micropuncture study of composition of proximal and distal tubular fluid in rat kidney. *Am J Physiol*. 1963; 204:527-531.

167. Van Abel M, Hoenderop JGJ, Van Der Kemp AWCM, *et al*. Coordinated control of renal Ca^{2+} transport proteins by parathyroid hormone. *Kidney Int*. 2005; 68(4):1708-1721. doi:10.1111/j.1523-1755.2005.00587.x.

168. Wallace RB, Wactawski-wende J, Sullivan MJO, *et al*. Urinary tract stone occurrence in the Women's Health Initiative (WHI) randomized clinical trial of calcium and vitamin D supplements 1 – 3. *Am J Clin Nutr*. 2011; 94(1):270-277. doi:10.3945/ajcn.110.003350.1.

169. Wang A, Li J, Zhao Y, *et al*. Loss of NHE8 expression impairs intestinal mucosal integrity. *Am J Physiol - Gastrointest Liver Physiol*. 2015; (520):ajpgi.00278.2015. doi:10.1152/ajpgi.00278.2015.

170. Wang T, Hropot M, Aronson PS, *et al*. Role of NHE isoforms in mediating bicarbonate reabsorption along the nephron. *Am J Physiol Renal Physiol*. 2001; 281(6):F1117-F1122.

171. Wang X, Takeya K, Aaronson PI, *et al*. Effects of amiloride, benzamil, and alterations in extracellular Na^+ on the rat afferent arteriole and its myogenic response. *Am J Physiol Renal Physiol*. 2008; 295(1):F272-F282. doi:10.1152/ajprenal.00200.2007.

172. Ward DT. Calcium receptor-mediated intracellular signalling. *Cell Calcium*. 2004; 35(3):217-228. doi:10.1016/j.ceca.2003.10.017.

173. Watson JF. Potassium reabsorption in the proximal tubule of the dog nephron. *J Clin Invest*. 1966; 45(8):1341-1348.

174. Weber K, Erben RG, Rump a, *et al*. Gene structure and regulation of the murine epithelial calcium channels ECaC1 and 2. *Biochem Biophys Res Commun*. 2001; 289(5):1287-1294. doi:10.1006/bbrc.2001.6121.

175. Wright F, Bomsztyk K. Calcium transport by the proximal tubule. *Adv Exp Med Biol*. 1986; 208:165-170.

176. Wu MS, Biemesderfer D, Giebisch G, *et al*. Role of NHE3 in mediating renal brush border Na^+/H^+ exchange: Adaptation to metabolic acidosis. *J Biol Chem*. 1996; 271(51):32749-32752. doi:10.1074/jbc.271.51.32749.

177. Xu H, Chen H, Li J, *et al*. Disruption of NHE8 expression impairs Leydig cell function in the testes. *Am J Physiol - Cell Physiol*. 2015; 308(4):C330-C338. doi:10.1152/ajpcell.00289.2014.

178. Xu H, Li J, Chen R, *et al*. NHE2X3 DKO mice exhibit gender-specific NHE8 compensation. *Am J Physiol Gastrointest Liver Physiol*. 2011; 300(4):G647-G653. doi:10.1152/ajpgi.00546.2010.

179. Xu H, Zhang B, Li J, *et al*. Impaired mucin synthesis and bicarbonate secretion in the colon of NHE8 knockout mice. *Am J Physiol Gastrointest Liver Physiol*. 2012; 303(3):G335-G343. doi:10.1152/ajpgi.00146.2012.

180. Xu H, Zhao Y, Li J, *et al*. Loss of NHE8 expression impairs ocular surface function in mice. *Am J Physiol Cell Physiol*. 2015; 308(1):C79-C87. doi:10.1152/ajpcell.00296.2014.

181. Yamaguchi T, Kifor O, Chattopadhyay N, *et al*. Extracellular calcium $(Ca^{2+})_o$ - sensing receptor in a mouse monocyte-macrophage cell line (J774): potential mediator of the actions of $(Ca^{2+})_o$ on the function of J774 cells. *J Bone Min Res*. 1998; 13(9):1390-1397. doi:10.1359/jbmr.1998.13.9.1390.

182. Yang L, Faraone S V., Zhang-James Y. Autism spectrum disorder traits in Slc9a9 knock-out mice. *Am J Med Genet Part B Neuropsychiatr Genet*. 2016; 171(3):363-376. doi:10.1002/ajmg.b.32415.

183. Yang TX, Hassan S, Huang YNG, *et al*. Expression of PTHrP, PTH/PTHrP receptor, and Ca^{2+}-sensing receptor mRNAs along the rat nephron. *Am J Physiol*. 1997; 272(21):F751-F758.

184. Yu H, Freedman BI, Rich SS, *et al*. Human Na^{+}/H^{+} Exchanger Genes. *Hypertension.* 2000; 35:135-143.

185. Yun CHC, Tse CM, Nath S, *et al*. Mammalian Na^{+}/H^{+} exchanger gene family: structure and function studies. *Am. J. Physiol.* 1995; 269(32):G1-G11.

186. Zhang J, Bobulescu IA, Goyal S, *et al*. Characterization of Na^{+}/H^{+} exchanger NHE8 in cultured renal epithelial cells. *Am J Physiol - Ren Physiol*. 2007; 293(3):F761-F766. doi:10.1152/ajprenal.00117.2007.

187. Zhang MIN, O'Neil RG. A regulated calcium channel in apical membranes of renal proximal tubule cells. *Am J Physiol*. 1996; 271:C1757-C1764.

188. Zuckerman JM, Assimos DG. Hypocitraturia: pathophysiology and medical management. *Rev Urol*. 2009; 11(3):134-144. doi:10.3909/riu0424.

APPENDIX

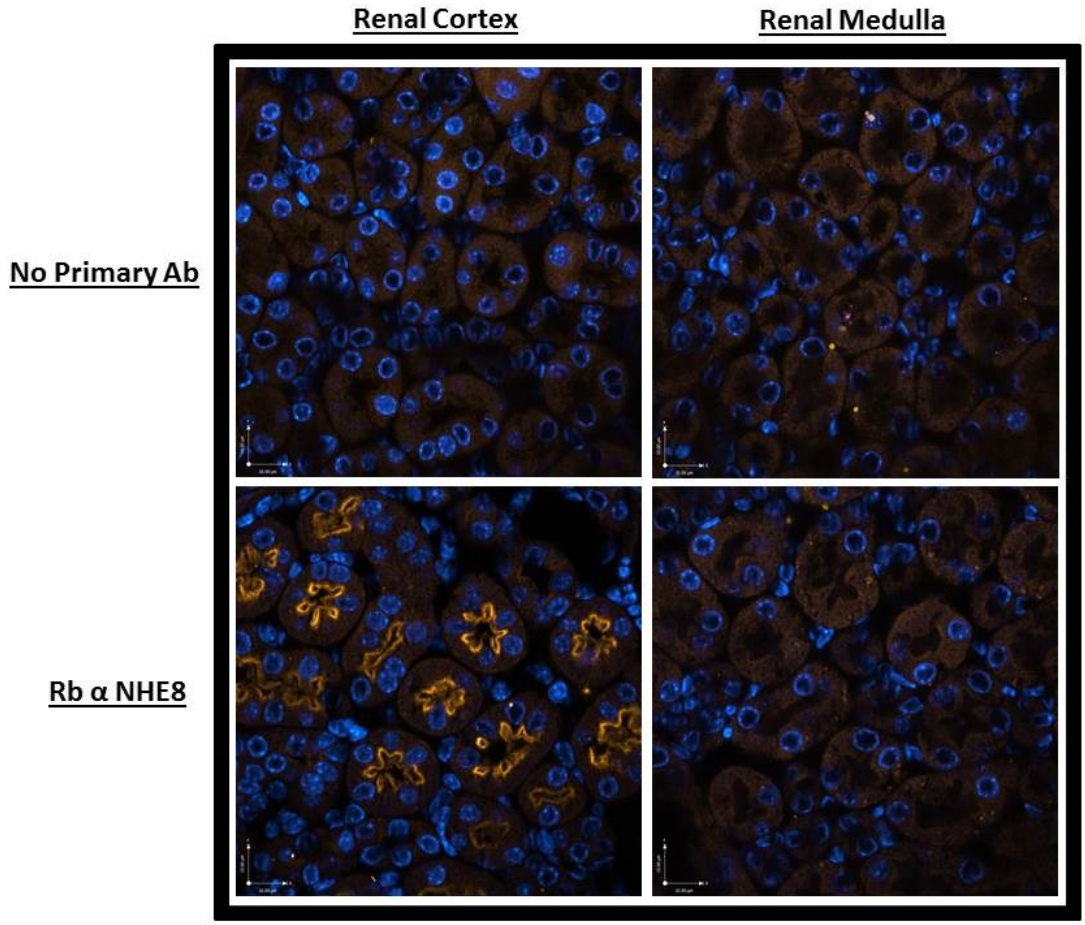

Rabbit anti-NHE8 polyclonal antibody specificity: Mouse kidney sections were analyzed using immunofluorescence as previously described. Images of the renal cortex and medulla were taken using confocal microscopy. The bottom panel images were taken from sections first probed with anti-NHE8 antibody and then with a secondary Cy3 conjugated antibody. The top panel images were taken from sections without anti-NHE8 primary antibody, but treated with secondary Cy3 conjugated antibody.

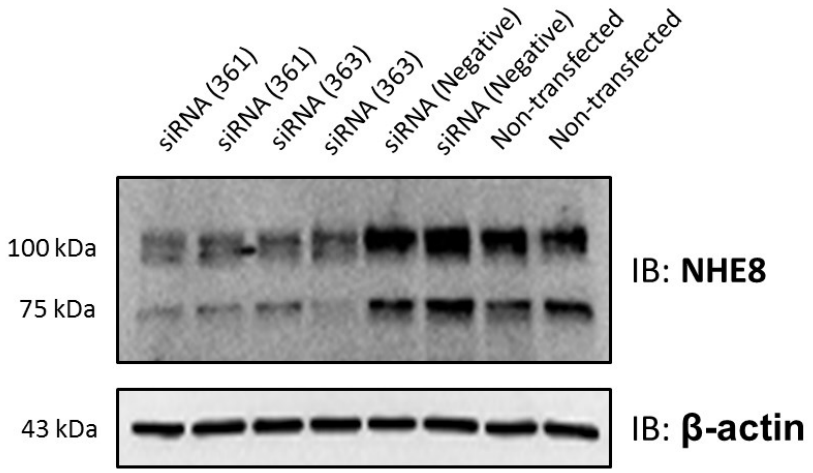

NHE8 protein expression is reduced in NRK cells treated with NHE8 specific siRNA. NRK cells were treated for 24 h with 100 nM of two siRNAs as described in materials and methods. siRNA negative is a scramble control and the non-transfected cells were subjected to oligofectamine reagent only. Experiment was performed in duplicates and β-actin was used as an internal loading control.

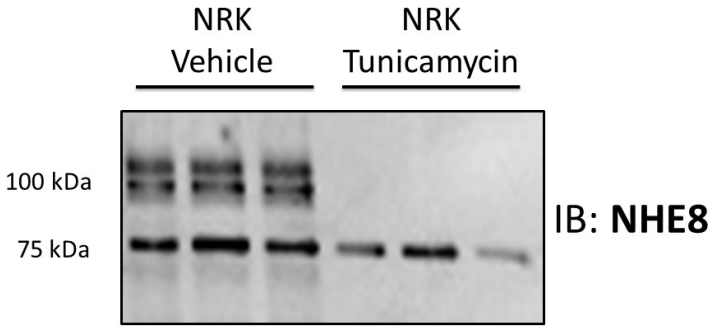

NRK cells treated with tunicamycin lose expression of glycosylated NHE8: N-acetylglucosamine transferase activity was inhibited in NRK cells via treatment with 5 µg/ml tunicamycin from Streptomyces for 32 h. Cell lysate was probed with anti-NHE8 (7A11).

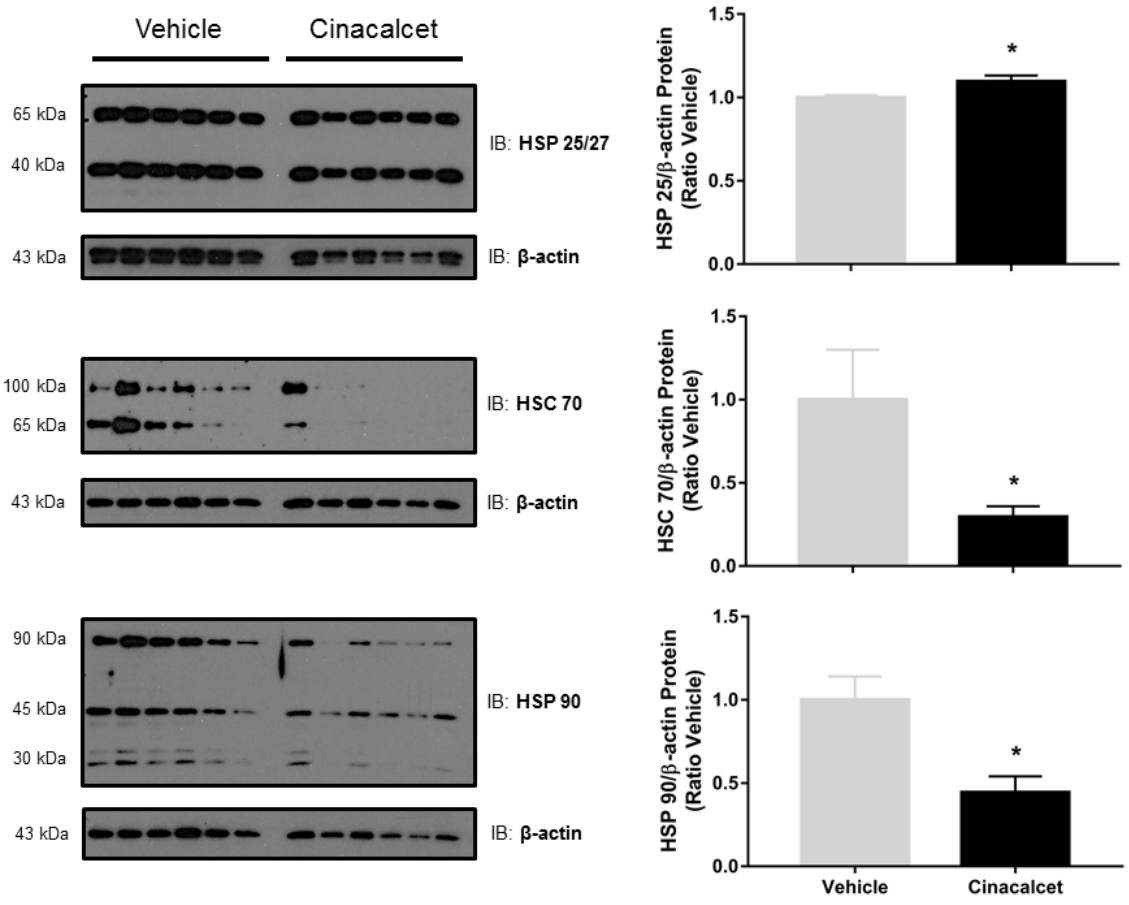

Renal heat shock protein expression in reduced is mice treated with cinacalcet: Kidney from mice treated with vehicle or cinacalcet were lysed and subjected to SDS-PAGE as previously described. Membranes were probed with primary antibodies against HSP 25/27, HSC 70, HSP 90 and β-actin as a loading control. Band intensity was normalized to β-actin and is shown as a ratio vehicle. N=6 for each group. Data are displayed as mean ± S.E *P<0.05.